

Carbon isotope evidence for the latitudinal distribution and wind speed
dependence of the air-sea gas transfer velocity

Nir Y. Krakauer^{1*}, James T. Randerson², François W. Primeau², Nicolas
Gruber³, Dimitris Menemenlis⁴

Submitted to *Tellus*
January 13, 2006

¹ Division of Geological and Planetary Sciences, California Institute of Technology,
Pasadena, CA 91125, USA

² Department of Earth System Science, University of California, Irvine, CA 92697, USA

³ IGPP & Department of Atmospheric and Oceanic Sciences, University of California,
Los Angeles, CA, 90095, USA

⁴ Jet Propulsion Laboratory, Pasadena, CA 91109, USA

* To whom correspondence should be addressed.

E-mail: niryk@caltech.edu

Phone: (626) 395-6271

The air-sea gas transfer velocity is an important determinant of the exchange of gases, including CO₂, between the atmosphere and ocean, but the magnitude of the transfer velocity and what factors control it remains poorly known. Here, we use oceanic and atmospheric observations of ¹⁴C and ¹³C to constrain the global mean gas transfer velocity as well as the exponent of its wind-speed dependence, utilizing the distinct signatures left by the air-sea exchange of ¹⁴CO₂ and ¹³CO₂. While the atmosphere and ocean inventories of ¹⁴CO₂ and ¹³CO₂ constrain the mean gas transfer velocity, the latitudinal pattern in the atmospheric and oceanic ¹⁴C and ¹³C distributions contains information about the wind speed dependence. We computed the uptake of bomb ¹⁴C by the ocean for different transfer velocity patterns using pulse response functions from an ocean general circulation model, and evaluated the match between the predicted bomb ¹⁴C concentrations and observationally based estimates for the 1970s-1990s. Using a windspeed climatology based on satellite measurements, we solved either for the mean gas transfer velocity over each of 11 ocean regions or for the best-fit global relationship between gas exchange and mean windspeed. We also compared the predicted consequences of different gas exchange relationships on the rate of change and interhemisphere gradient of ¹⁴C in atmospheric CO₂ with tree-ring and atmospheric measurements. Our results suggest that globally, the dependence of the air-sea gas transfer velocity on windspeed is close to linear, with an exponent of 0.9 ± 0.4 , and that the global mean gas transfer velocity at a Schmidt number of 660 is 21 ± 2 cm / hour, similar to the results of previous analyses. We find that the air-sea flux of ¹³C estimated from

atmosphere and ocean observations also suggests a lower than quadratic global dependence of gas exchange on windspeed.

Introduction

In recent decades, the ocean has absorbed roughly one third of the CO₂ released into the atmosphere by fossil fuel burning [*Prentice et al.*, 2001; *Sabine et al.*, 2004]. Ocean CO₂ uptake thus significantly influences the course of greenhouse climate forcing. Further, the added CO₂ makes the ocean more acidic, with potentially serious consequences for ocean ecology [*Caldeira and Wickett*, 2003; *Feely et al.*, 2004a; *Orr et al.*, 2005]. As a result, quantitative description of the air-sea CO₂ flux and of changes in ocean carbon chemistry has become a leading goal of oceanographic research [e.g. *Fasham*, 2003].

The air-sea flux of CO₂ and other gases is generally estimated using a bulk parameterization approach, i.e. assumed to be proportional to the difference in the concentration of a gas between the bulk ocean and the bulk atmosphere [e.g. *Liss and Merlivat*, 1986; *Frost and Upstill-Goddard*, 1999; *Orr et al.*, 2001]. This implies a relationship of the form

$$F = k_w \cdot (C_s - C_a), \quad (1)$$

where F is the gas flux out of the ocean (with units such as $\text{mol m}^{-2} \text{s}^{-1}$); C_s is the gas concentration in surface water (mol m^{-3}); C_a is the surface ocean concentration of the gas

in equilibrium with the partial pressure p (atm) of the gas in the air over the ocean surface computed from Henry's law, i.e. $C_a = \alpha \cdot p$, with α ($\text{mol m}^{-3} \text{ atm}^{-1}$) being the gas solubility; and k_w is an air-sea gas transfer velocity (m s^{-1}) that is independent of the gas concentration but might depend on, for example, the gas diffusivity and sea surface state. In this bulk parameterization, a negative concentration gradient $C_s - C_a$ across the air-sea interface is the driving force for gas uptake by the ocean, but the instantaneous uptake rate then depends on the gas transfer velocity k_w .

Knowledge of the gas transfer velocity is vital to approaches that estimate contemporary ocean CO_2 uptake from observations of the air-sea pCO_2 disequilibrium [Takahashi *et al.*, 2002] as any bias or uncertainty in the gas transfer velocity leads to a corresponding bias or uncertainty in the flux estimate. The gas transfer velocity is also a very important input parameter for the estimation of the oceanic uptake of anthropogenic CO_2 using an isotopic budget of ^{13}C in the atmosphere and ocean [Tans *et al.*, 1993; Gruber and Keeling, 2001; Quay *et al.*, 2003]. Knowledge of the gas transfer velocity is of secondary importance for modeling the air-sea exchange of CO_2 , except at regions where vertical mixing is rapid, such as the equator and at high latitudes, where surface water turns over too quickly to reach equilibrium with atmospheric gas pressures [England *et al.*, 1994; Murnane *et al.*, 1999; Ito *et al.*, 2004]. Accurate determination of the gas transfer velocity would also help in inferring the air-sea fluxes of a variety of other gases of biogeochemical interest, such as oxygen, nitrous oxide, and dimethyl sulfide, from measurements of the concentration gradient across the air-sea interface [e.g. Liss *et al.*, 2004].

Gas transfer velocities over periods of up to a few days have been measured in laboratory wind tunnels as well as in small lakes and in the ocean [overviews in *Jähne and Haussecker, 1998; Frost and Upstill-Goddard, 1999*]. Methods used include eddy correlation for fluxes of gases such as CO₂ [*McGillis et al., 2001*], and observing the evasion of purposefully released tracer gases such as SF₆ and helium-3 [*Nightingale et al., 2000*]. Gas transfer velocities are found to depend on boundary layer turbulence and to be enhanced by the formation of bubbles from breaking waves [see *Asher et al., 1998*], and in many cases can be related to prevailing windspeed.

Drawing on such findings, *Wanninkhof* [1992] proposed a formulation for the air-sea gas transfer velocity that depends quadratically on windspeed,

$$k_w = k_0 \cdot u^2 \cdot (Sc/660)^{-0.5}, \quad (2)$$

where k_0 is a constant, u is the windspeed measured at 10-meter height (m s^{-1}), and Sc is the Schmidt number (water kinematic viscosity divided by the gas diffusivity). 660 is a scaling factor included for convenience because it is a typical value for the Schmidt number of CO₂ in the ocean. The exponent -0.5 is representative of the diffusivity dependence found in various laboratory dual-tracer experiments, and more recently also in the open ocean [*Nightingale et al., 2000*]. *Wanninkhof* [1992] calibrated the constant k_0 such that the global mean gas transfer velocity is consistent with the mean gas transfer velocity estimated from natural [*Broecker and Peng, 1982*] and bomb ¹⁴C [*Broecker et al., 1986*] (see more below).

The *Wanninkhof* [1992] formulation has been widely adopted for estimating ocean uptake of CO₂ and other gases from an observed or modeled air-sea concentration difference [e.g. *England et al.*, 1994; *Orr et al.*, 2001; *Dutay et al.*, 2002; *Takahashi et al.*, 2002]. Earlier, a linear, or piecewise linear, dependence on windspeed was more commonly assumed [*Broecker et al.*, 1985; *Liss and Merlivat*, 1986; *Toggweiler et al.*, 1989; *Tans et al.*, 1990]. *Wanninkhof and McGillis* [1999] more recently suggested that gas exchange may scale with the cube, rather than the square, of windspeed.

Comparing the commonly used relationships between air-sea gas exchange and windspeed proposed by *Wanninkhof* [1992], *Wanninkhof and McGillis* [1999] and others such as *Liss and Merlivat* [1986] and *Nightingale et al.* [2000] reveals a range of at least a factor of 2 at any given windspeed. This leads directly to a factor of 2 uncertainty in the air-sea flux when estimated from air-sea partial pressure difference. The different relationships also lead to rather different diagnosed latitudinal pattern of air-sea fluxes in contemporary CO₂ because of the large mean differences in windspeed (Figure 1). If the gas transfer velocity increases as a quadratic or cubic power of windspeed even under high winds, much of the total ocean CO₂ uptake may be occurring during sporadic intense storms, such as hurricanes, and interannual variability in storm frequencies could explain much of the observed interannual variability in the rate of increase of atmospheric CO₂ [*Bates*, 2002], although inferences from atmospheric O₂ and δ¹³CO₂ do not support assigning such great interannual variability to the ocean CO₂ sink [*Bousquet et al.*, 2000]. Formulations of the air-sea gas transfer velocity thus need further evaluation.

In this study, we explore how observations of ^{14}C and ^{13}C in the atmosphere and ocean can help to constrain the mean gas exchange velocity as well as the exponent n of the windspeed dependency. Some of the ^{14}C constraints are well known and have been used previously, but we also introduce a set of new constraints, such as the interhemisphere gradient in the atmospheric ^{14}C content and the rate of decrease in atmospheric ^{14}C . We further consider how the measurements of ^{13}C and its air-sea isotope flux can be used to address this question, supplementing the ^{14}C constraints. The next section introduces these constraints and how they have been used in the past.

Carbon isotope constraints on the gas transfer velocity

Observations of carbon-14 (radiocarbon) concentrations in the atmosphere and ocean have played a very important role in constraining the gas transfer velocity. ^{14}C is an unstable isotope with a half-life of 5730 years which comprises about one part in 10^{12} of the carbon in earth's atmosphere. ^{14}C is produced in the upper atmosphere at a roughly steady rate in reactions with cosmic rays and solar protons [e.g. *Lingenfelter*, 1963]. From there, it is transported as $^{14}\text{CO}_2$ into the lower atmosphere and then taken up by the ocean and terrestrial biosphere. Because water from the deep ocean takes on the order of 1000 years to circulate to the surface, dissolved inorganic carbon (DIC) in the deep ocean typically has a $^{14}\text{C}/^{12}\text{C}$ ratio about 200‰ lower than the atmospheric concentration [e.g. *Nydal*, 2000]. Surface ocean DIC reflects exchange both with the deep ocean and with the atmosphere, and so has an intermediate ratio.

The uptake of $^{14}\text{CO}_2$ by the ocean is relatively slow. A mixed layer of 50 m depth takes roughly 10 years for its DIC ^{14}C content to reach equilibrium with a perturbation in the $^{14}\text{CO}_2$ content of the overlying air [Broecker and Peng, 1982]. This equilibration time-scale is longer than the typical residence time of water in the surface mixed layer, leading to the observation that the surface ocean ^{14}C content of DIC can be far from equilibrium with the atmosphere (large concentration gradients across the air-sea interface). This contrasts strongly with the exchange of other gases, including oxygen and chlorofluorocarbons, whose exchange time-scale is of the order of a week, resulting in surface ocean concentrations usually being very close to their equilibrium concentration.

^{14}C isotopic abundance is expressed in delta notation, where $\Delta^{14}\text{C}$ is the ratio of the measured $^{14}\text{C}/^{12}\text{C}$ ratio (normalized for mass-dependent isotopic fractionation to a reference $^{13}\text{C}/^{12}\text{C}$ level) to that of atmospheric CO_2 in the 19th century (determined from tree ring cellulose carbon), minus one [Stuiver and Polach, 1977]. Tree ring records show that $\Delta^{14}\text{C}$ of atmospheric CO_2 (or “atmospheric $\Delta^{14}\text{C}$ ”) remained close to 0‰ in the centuries prior to the 20th century, suggesting that the global carbon cycle remained in an approximate steady-state [Stuiver and Becker, 1993], while measurements of coral carbonate show that surface water DIC averaged around -50‰ [Druffel and Suess, 1983]. In the first half of the 20th century, atmospheric $\Delta^{14}\text{C}$ dropped by around 20‰ because of dilution of ^{14}C by CO_2 derived from fossil fuels, which contain no ^{14}C [Suess, 1955; Tans *et al.*, 1979; Stuiver and Quay, 1981].

Nuclear bomb tests in the 1950s and early 1960s produced large amount of ^{14}C (“bomb radiocarbon”) in the upper atmosphere, so that $\Delta^{14}\text{C}$ of CO_2 in the lower troposphere rose to $+800\text{‰}$ by 1964, only to decline in the following decades (to around

+65‰ in 2004) as a result of exchange of atmospheric carbon with biosphere and ocean reservoirs that had lower $\Delta^{14}\text{C}$ (Figure 2a). The bomb radiocarbon influx from the atmosphere into the surface ocean increased the $\Delta^{14}\text{C}$ of surface water DIC as much as 300‰ by 1970 [Linick, 1980] (Figure 2b), at a rate set by air-sea gas exchange, and this bomb radiocarbon is now spreading into deeper water [e.g. Broecker *et al.*, 1985; Masiello *et al.*, 1998]. Due to the long equilibration time-scale of $^{14}\text{CO}_2$ across the air-sea interface, ocean bomb $^{14}\text{CO}_2$ uptake is strongly limited by air-sea exchange, making the bomb $^{14}\text{CO}_2$ inventory a powerful constraint for the gas transfer velocity.

The first extensive set of measurements of $\Delta^{14}\text{C}$ of ocean DIC (or “ocean $\Delta^{14}\text{C}$ ”) was made as part of the Geochemical Ocean Sections (GEOSECS) program. In a series of oceanographic cruises in 1972-1978, $\Delta^{14}\text{C}$ profiles were measured at about 100 locations, clearly showing the enhancement of $\Delta^{14}\text{C}$ in surface water due to bomb radiocarbon as well as elucidating deep water circulation pathways [Ostlund and Stuiver, 1980; Stuiver and Ostlund, 1980; 1983].

Broecker *et al.* [1985; 1986; 1995] used the GEOSECS data to estimate the ocean bomb radiocarbon inventory by latitude band, arriving at $305 \pm 30 \times 10^{26}$ atoms in the whole ocean as of the beginning of 1975 (“mid-GEOSECS”). Based on this inventory, Broecker *et al.* estimated the global mean CO_2 invasion rate (equivalent to the product $k_w C_a$ in our notation [Equation 1]) at $20 \pm 3 \text{ mol m}^{-2} \text{ year}^{-1}$, a rate also consistent with pre-bomb ocean $\Delta^{14}\text{C}$ profiles [Broecker and Peng, 1982]. Broecker and Peng [1982] used GEOSECS and other ^{14}C data to also look at the natural ^{14}C constraint on the gas transfer velocity. This constraint arises from the requirement that at steady state, the net invasion of $^{14}\text{CO}_2$ into the ocean must be balanced by the decay of ^{14}C in the ocean. By subtracting

the estimated bomb ^{14}C from the observed ^{14}C , *Broecker and Peng* [1982] obtained an estimate of the total ^{14}C that existed in the ocean in preindustrial times and an estimate of the preindustrial air-sea difference in $\Delta^{14}\text{CO}_2$, from which they derived an estimate of the gas transfer velocity. The estimate *Broecker and Peng* [1982] obtained following this approach was remarkably close to that obtained from the bomb ^{14}C constraint. These ^{14}C -based mean values have since then been widely used [e.g., *Tans et al.*, 1990; *Wanninkhof*, 1992; *Wanninkhof and McGillis*, 1999] to set the scaling factor k_0 in expressions for k_w as a function of windspeed (such as Equation 2).

Hesshaimer et al. [1994] attempted to deduce from stratospheric $\Delta^{14}\text{C}$ measurements the total amount of bomb radiocarbon produced and to derive a consistent budget for its spread. They found that atmospheric $\Delta^{14}\text{C}$ had been declining more slowly than would be expected given the GEOSECS-derived rate of ocean uptake and assumptions about biosphere carbon uptake. They therefore proposed that mid-1970s ocean bomb radiocarbon uptake had to be $\sim 25\%$ lower, or around 230×10^{26} atoms, and suggested that this implies a lower mean gas transfer velocity.

Peacock [2004] showed that simple extrapolation of the GEOSECS station inventories to the whole ocean likely results in an overestimate of the GEOSECS inventory. She obtained an inventory of $258 \pm 50 \times 10^{26}$ atoms using multiple linear regression of GEOSECS radiocarbon measurements against well-measured ocean quantities, and some $270 \pm 25 \times 10^{26}$ atoms for the beginning of 1975 using modeled ocean CFC and anthropogenic CO_2 concentration fields to adjust the *Broecker et al.* [1995] extrapolation from GEOSECS measurements. This adjustment can be expected to affect the implied mean gas transfer velocity.

In the 1980s and especially the 1990s, the World Ocean Circulation Experiment (WOCE) and affiliated oceanographic survey programs measured ocean $\Delta^{14}\text{C}$ at many more locations, increasing the number of available data by an order of magnitude [Key *et al.*, 2002]. In this paper, we use both GEOSECS results and these new data together with an ocean circulation model to evaluate the mean air-sea transfer velocity and the form of its dependence on windspeed implied by ocean bomb ^{14}C uptake. We also revisit the natural ^{14}C constraint developed by Broecker and Peng [1982]. In addition, we explore three other ^{14}C constraints, all arising from observations of atmospheric ^{14}C .

The first constraint pertains to the preindustrial interhemispheric gradient of ^{14}C . As a result of the upwelling of very old waters with low $\Delta^{14}\text{C}$ in the Southern Ocean, the ^{14}C content in the surface waters of the Southern Ocean is the lowest anywhere, leading to the largest air-sea gradient in ^{14}C . Taken together with the high windspeeds prevailing in this region, this means that the Southern Ocean takes up a disproportionately large amount of ^{14}C from the atmosphere. This is believed to be the major reason that atmospheric $\Delta^{14}\text{C}$ was a few permil lower in the southern than in the northern hemisphere in preindustrial times, as inferred from measurements of tree rings [Braziunas *et al.*, 1995]. This atmospheric gradient is sensitive to latitudinal variation in the air-sea transfer velocity, while the overall rate of preindustrial ocean ^{14}C uptake is sensitive primarily to the global mean transfer velocity [Broecker and Peng, 1982].

The second and third additional ^{14}C constraints pertain to the post-bomb period. Since the 1980s, the low-latitude oceans have grown close to isotopic equilibrium with the declining atmospheric $\Delta^{14}\text{C}$ level [e.g. Caldeira *et al.*, 1998], leaving the Southern Ocean, which still has low surface $\Delta^{14}\text{C}$ due to extensive mixing with deeper waters, as

the major site of the uptake of bomb ^{14}C by the ocean [Levin *et al.*, 1987; Randerson *et al.*, 2002]. Thus, recent measurements of both the rate of decline in atmospheric $\Delta^{14}\text{C}$ and the atmospheric $\Delta^{14}\text{C}$ gradient between the tropics and high southern latitudes should be particularly sensitive to the air-sea transfer velocity over the Southern Ocean, providing constraints on the parameters \bar{k} and n .

We also consider whether what is known about the total global air-sea fluxes of carbon-13 can help in inferring the form of the gas transfer velocity, as suggested by Heimann and Monfray [1989]. ^{13}C has the same slow exchange time-scale that characterizes ^{14}C . This has resulted in the surface ocean $^{13}\text{C}/^{12}\text{C}$ ratio lagging substantially behind the recent decrease in the atmospheric $^{13}\text{C}/^{12}\text{C}$ ratio arising from the burning of fossil fuels with a low $^{13}\text{C}/^{12}\text{C}$ ratio [e.g., Bacastow *et al.*, 1996]. As a consequence, there is now a large net ^{13}C isotope flux out of the ocean. However, isotopic fractionation associated with photosynthesis leads to a distinct latitudinal pattern in $^{13}\text{C}/^{12}\text{C}$ of ocean DIC, so that there is an isotope flux out of the ocean at low latitudes but into the ocean at high latitudes [Gruber *et al.*, 1999]. Thus, given the observed surface ocean $^{13}\text{C}/^{12}\text{C}$ ratio of DIC, a stronger increase of the gas transfer velocity with windspeed implies a smaller exchange-weighted ^{13}C isotope flux out of the ocean. This can be compared with the ^{13}C isotope flux required to match observations of the rate of change in the $^{13}\text{C}/^{12}\text{C}$ ratio of atmospheric CO_2 and of ocean DIC [Heimann and Maier-Reimer, 1996; Gruber and Keeling, 2001; Quay *et al.*, 2003]. A second ^{13}C constraint exists in the preindustrial ^{13}C flux, which arises from the input of isotopically light organic carbon by rivers, which is then mostly remineralized in the ocean. This flux has been estimated to be of the order of 0.4 Pg C / year [Heimann and Maier-Reimer, 1996;

Aumont et al., 2001]. We compare this steady-state preindustrial ^{13}C isotope flux with that calculated from the estimated preindustrial $^{13}\text{C}/^{12}\text{C}$ ratio of the atmosphere and of sea-surface DIC; given the strong latitudinal dependence of the air-sea gradient in the $^{13}\text{C}/^{12}\text{C}$ ratio, this calculated flux would depend sensitively on the assumed windspeed dependence of the gas transfer velocity.

In combining these multiple carbon-14 and carbon-13 constraints, we first present results for simulations of ocean uptake of bomb ^{14}C using an ocean transport model, which we compare with compiled measurements of bomb ^{14}C in the ocean, and with published estimates, based on these measurements, of the total amount and distribution of bomb ^{14}C in the ocean at the 1970s and 1990s (the time of GEOSECS and WOCE respectively). Using this evidence, we find the range of global mean transfer velocities and power law dependences of the transfer velocity on windspeed that best explain the measured distribution. We then check this proposed relationship of the gas transfer velocity with windspeed against other observations of ^{14}C in the atmosphere and of ^{13}C in the ocean and atmosphere. The comparisons with the observed latitudinal distribution of atmospheric $\Delta^{14}\text{C}$ require the use of an atmospheric transport model to estimate the atmospheric latitudinal gradients that would result from different possible air-sea flux patterns. Our overall goal is to learn from ocean and atmosphere ^{14}C and ^{13}C observations about the mean gas transfer velocity over timescales of months to decades and its regional variability. This would complement smaller-scale laboratory and field work in suggesting and testing parameterizations for air-sea gas exchange.

Methods

Ocean circulation models

To efficiently simulate the uptake of bomb ^{14}C for many different scenarios, we employed a substitute model derived from surface pulse response functions (see *Joos* [1996] and *Gloor et al.* [2001] for the concept). We used regional pulse functions derived from the MIT general circulation model (MITgcm) [*Marshall et al.*, 1997] integrated in a quasi-global (80°S to 80°N) ocean configuration with 1° horizontal grid spacing and with 23 vertical levels. This model was driven by air-sea fluxes of heat, freshwater, and momentum derived by the consortium for Estimating the Circulation and Climate of the Ocean (ECCO) for the 1992-2002 period using the “adjoint” method to fit the model to a wide variety of satellite and *in situ* observations [*Stammer et al.*, 2004]. This ocean model was used to compute tracer Green’s functions for estimating anthropogenic CO₂ uptake, as described by *Mikaloff Fletcher et al.* [in press]. All configuration details were as in *Stammer et al.* [2004], except that (i) the 1992-2002 surface boundary conditions were repeated in order to cover the 1765-2005 simulation period, (ii) sea surface salinity was relaxed to a monthly mean climatology from the National Oceanographic Data Center (NODC) World Ocean Atlas 1998 (WOA98) with a time constant of 30 days, and (iii) sea surface temperature was relaxed to daily mean 1992-2002 estimates from the National Centers for Environmental Prediction and the National Center for Atmospheric Research (NCEP/NCAR) atmospheric reanalysis, also with a time constant of 30 days. This model configuration has been found to reproduce the CFC distribution measured during the 1990s WOCE cruises better than any of the other ocean models compared in the Ocean

Carbon-Cycle Model Intercomparison Project (OCMIP) Phase 2 study [Dutay *et al.*, 2002; Mikaloff Fletcher *et al.*, in press]. We deconvolved regional pulse response functions for the MITgcm from the tracer Green's functions computed for the Mikaloff Fletcher *et al.* [in press] study. Given the known flux boundary conditions, we transformed these Green's functions to obtain pulse-response functions describing yearly mean concentration patterns resulting from an instantaneous unit pulse of a tracer into each of 30 surface basis regions (shown in Figure 3a). We then used the pulse response substitute model to simulate the time-varying bomb radiocarbon distributions resulting from a given gas transfer velocity pattern.

To check for errors in model transport, and to assess the degradation in accuracy caused by using the substitute model instead of the full ocean circulation model, we simulated ocean uptake of the chlorofluorocarbons CFC-11 and CFC-12 with the same substitute model and compared the modeled fields with WOCE ocean observations and with a simulation using the full MITgcm. Our boundary conditions followed the OCMIP protocol for chlorofluorocarbons [Dutay *et al.*, 2002], and we used the standard OCMIP air-sea gas exchange formulation. Our substitute model simulated 1994 CFC-11 inventory was 11% lower than that of the gridded field based on WOCE measurements [Key *et al.*, 2004] – 4.61×10^8 versus 5.16×10^8 mol for the volume covered by the gridded field – and the modeled latitudinal distribution tracked the observed one very well, with the exception of underestimating uptake in the northern subtropics (Figure 4). (The estimated uncertainty in the WOCE gridded inventory is 15%, or 0.8×10^8 mol [Key *et al.*, 2004].) The latitudinal distribution was also close to that simulated using the full MITgcm (Figure 4), suggesting that simulations using the substitute model preserve the

large-scale features simulated using the full transport model. Using the substitute model, the correlation coefficient between individual ocean CFC measurements in the GLODAP database [Key *et al.*, 2004] and the modeled CFC concentration at the same grid box and month was +0.84. (The full model corresponded better with observations, with a correlation coefficient of +0.92; its simulated 1994 CFC-11 inventory was 4.82×10^8 mol.) Results for CFC-12 were similar, with the ocean inventory underestimated by 8% and a measured-modeled correlation coefficient of +0.85 using the pulse functions.

Calculation of the perturbation in sea-surface $\Delta^{14}\text{C}$ caused by the pre-bomb decrease in $\Delta^{14}\text{C}$ of atmospheric CO_2 attributable to fossil fuel burning, and the perturbation in the sea-surface $^{13}\text{C}/^{12}\text{C}$ ratio caused by the ongoing decrease in the $^{13}\text{C}/^{12}\text{C}$ of atmospheric CO_2 , also attributable to fossil fuel burning, required longer integration times than those available in our pulse response substitute model. For these calculations, we used an offline version of an ocean general circulation model, with monthly-mean transport fields obtained from a version of the Modular Ocean Model (MOM) [Pacanowski *et al.*, 1993] configured as described by Primeau [2005]. This model overpredicted rather than underpredicted the 1990s ocean CFC inventory, due to excessive uptake in the Southern Ocean (Figure 4): the modeled 1994 inventory was 5.97×10^8 mol, 16% above the inventory based on WOCE measurements. The modeled-measured correlation coefficient for individual CFC-11 measurements was +0.86. Because the MITgcm latitudinal CFC uptake pattern matched observations more closely overall, we used the MITgcm pulse functions to simulate of ocean bomb ^{14}C uptake.

Atmospheric transport model

To predict the gradients in atmospheric $\Delta^{14}\text{C}$ resulting from various air-sea gas exchange patterns combined with other carbon fluxes, we again used regional pulse functions for their computational speed and accuracy. These atmospheric pulse response functions, which compactly represent the effect of the release of a unit amount of inert tracer at the surface in a particular region on the atmospheric concentration pattern of that tracer [e.g. *Randerson et al.*, 2002], were generated using the Model of Atmospheric Transport and Chemistry (MATCH) [*Mahowald et al.*, 1997]. MATCH was run with approximately 5.5° horizontal resolution and 26 vertical levels, and driven by meteorological fields from the NCAR Community Climate Model Version 3 [*Olsen and Randerson*, 2004]. Our pulse functions corresponded to tracer releases over the 22 TransCom regions [*Gurney et al.*, 2002] over each month of the year, allowing us to accurately represent seasonally varying fluxes. We also constructed pulse functions for northern, southern, and equatorial tracer release in the stratosphere (at the 90 millibar pressure level) and in the upper troposphere (at 200 millibar) to allow us to simulate the effect of cosmogenic ^{14}C production in the upper atmosphere on atmospheric $\Delta^{14}\text{C}$ gradients.

To estimate the error in modeling atmospheric transport with our pulse functions, we compared the latitudinal $\Delta^{14}\text{C}$ gradients modeled for several of our flux fields with those predicted by annual-mean regional pulse functions generated from an ensemble of 15 transport models for the TransCom Level 3 experiment [*Gurney et al.*, 2003]. Our model predictions were generally within one standard deviation of the intermodel mean.

We used the intermodel standard deviation as an estimate of the error in the predicted gradients induced by our atmospheric transport model.

The assumed functional form of the air-sea gas transfer velocity

We took as our reference the parameterization suggested by *Wanninkhof* [1992], which involves a quadratic dependence on windspeed and was scaled to yield the ^{14}C -derived global mean gas transfer velocity (Equation 2). Following OCMIP Phase 2, we use monthly distributions of root-mean-square windspeed over the ocean derived from Special Sensor Microwave Image (SSM/I) satellite measurements over the period 1988-1993 [*Boutin and Etcheto*, 1996] (shown in Figure 1) as the basis for estimating u^2 . Below, we will generally refer to this distribution of the gas transfer velocity simply as the *Wanninkhof* [1992] distribution. The global mean gas transfer velocity implied by this parameterization, averaged over ice-free water, is 20.6 cm / hour (at a Schmidt number of 660).

To test whether the *Wanninkhof* [1992] formulation is consistent with data on air-sea carbon isotope exchange, and to determine, if necessary, a more suitable formulation, we sought to estimate the global mean transfer velocity \bar{k} and the windspeed dependence exponent n in the relationship

$$k_w = \bar{k} \left(\frac{u^n}{u^n} \right) (\text{Sc}/660)^{-0.5} \quad (3)$$

where we used the root mean square climatological windspeed used in OCMIP (varying in space and monthly) as an estimate of u and where $\overline{u^n}$ is the area-weighted global mean of a power of windspeed (spatially and seasonally constant for a given value of n). (Dividing by $\overline{u^n}$ holds the area-weighted global mean transfer velocity at \overline{k} regardless of the value of n chosen.) To estimate the parameters \overline{k} and n , we compared the modeled isotope distributions calculated using different values of \overline{k} and n in Equation 4 with available observations and sought values of \overline{k} and n that yielded ocean carbon-14 or carbon-13 uptake patterns that agreed well with the observations. We considered values of \overline{k} ranging from 0.5 to 1.5 times the *Wanninkhof* [1992] value, or 10-31 cm / hour, and values of n ranging from 0 to 3. As detailed in the next sections, we employed several largely independent approaches, using different sets of observations and different applications of our atmosphere and ocean transport models.

Estimating the gas transfer velocity from ocean bomb ^{14}C

Simulating ocean uptake of bomb ^{14}C

Following the simplified formulation of *Toggweiler et al.* [1989], we carried bomb radiocarbon in Δ units, and it entered the surface layer following a version of Equation 1 appropriate for isotope fluxes, namely

$$F = k_w \cdot \alpha \cdot p\text{CO}_2 \cdot (\Delta_{\text{sea}}^{14}\text{C} - \Delta_{\text{air}}^{14}\text{C}) / \text{DIC}, \quad (4)$$

where F is now the air-sea flux in Δ units m s^{-1} (positive when out of the ocean), k_w is the gas transfer velocity for CO_2 in m s^{-1} , α is the solubility of CO_2 in seawater ($\text{mol m}^{-3} \text{atm}^{-1}$), $p\text{CO}_2$ is the partial pressure of CO_2 in the air (atm), $\Delta_{\text{sea}}^{14}\text{C}$ is the bomb carbon-14 content of sea surface DIC in Δ units, $\Delta_{\text{air}}^{14}\text{C}$ is the carbon-14 content of atmospheric CO_2 in Δ units above the preindustrial level of 0‰, and DIC is the sea surface DIC concentration (mol m^{-3}).

The uptake of bomb ^{14}C by the ocean was then computed by combining the flux boundary condition (Eq. 4) with the substitute model representing the transport of bomb ^{14}C into the ocean interior. Our bomb radiocarbon simulations began in 1956 with an ocean bomb radiocarbon concentration initialized at zero (following the operational definition of bomb radiocarbon used in *Rubin and Key* [2002]) and then stepped forward in time.

Of the terms on the right hand side of Equation 4, we varied k_w as specified below. $\Delta_{\text{sea}}^{14}\text{C}$ was the model prediction for the end of the previous time step. Values for the other terms were adapted from those used in various OCMIP tracer uptake studies, as follows. α was calculated based on the relationship of *Weiss and Price* [1980] and monthly climatological water surface temperature and salinity from the World Ocean Atlas 2001 [*Boyer et al.*, 2002; *Stephens et al.*, 2002]. $p\text{CO}_2$ was estimated from a time series of annual-mean CO_2 mixing ratios based on measurements at Mauna Loa (http://quercus.igpp.ucla.edu/OceanInversion/inputs/atm_co2/splco2_mod.dat) [*Keeling et al.*, 1976] and a monthly climatology of sea-level atmospheric pressure from *Esbensen and Kushnir* [1981]. $\Delta_{\text{air}}^{14}\text{C}$ was from a compilation of annual mean values for northern, equatorial and southern latitudes (I. Levin, personal communication to J. Orr,

http://www.ipsl.jussieu.fr/OCMIP/phase3/simulations/NOCES/boundcond/atmC14/Levin/Jim_data_2004.doc) based on long-term atmospheric measurement series at several sites [e.g. *Rozanski et al.*, 1995; *Levin and Kromer*, 2004]. DIC was based on climatologies produced by the Global Ocean Data Analysis Project (GLODAP) for the 1990s (from extensive oceanographic observations) and preindustrially (by subtracting an estimated anthropogenic component from the observations [*Gruber et al.*, 1996]) [*Key et al.*, 2004]. We interpolated between the preindustrial period and the 1990s by assuming that the amount of anthropogenic DIC in the ocean is everywhere proportional to the atmospheric CO₂ mixing ratio elevation above the preindustrial level at the current time step. The comparatively small share of anthropogenic DIC during the simulation period (generally less than 3% of total DIC, even at the surface) means that any errors induced by this interpolation scheme are small.

We applied Equation 4 to ice-free water. We assumed that no gas exchange occurs across sea ice, defined by a monthly sea ice climatology based on *Walsh* [1978] and *Zwally et al.* [1983].

Varying the air-sea gas transfer velocity

We took two different approaches for varying the *Wanninkhof* [1992] gas transfer velocity to fit ocean bomb radiocarbon observations. In the first approach, we solved for the best-fit mean transfer velocity in each of 11 large ocean regions, which were aggregations of the 30 ocean regions for which we had pulse functions and were very similar to the basis regions of the TransCom study [*Gurney et al.*, 2002]. We successively

perturbed the transfer velocity for each region from the *Wanninkhof* [1992] global mean by a fractional amount (generally 0.1) to construct a linear operator that represented the effect of varying the mean gas transfer velocity in each region on the amounts of bomb radiocarbon simulated at the measurement locations and months. This linearization made it easier to estimate the regional transfer velocities that minimized the misfit between simulated and observed values (with misfit functions as described below). Since the nonlinearity of the dependence of simulated concentrations and inventories on the air-sea transfer velocity was weak, iterating this linearization about the regional transfer velocities estimated from the previous iteration led to rapid convergence. This approach is conceptually similar to that of *Gloor et al.* [2001; 2003] and *Gruber et al.* [2001], who solved for regional air-sea fluxes of heat, oxygen, or anthropogenic CO₂ that best fit ocean observations. As a final step, we fit a power law to the relationship of the derived regional gas transfer velocities with regional mean windspeeds to estimate globally optimal values for \bar{k} and n .

Our second approach similarly fit air-sea exchange parameters to bomb radiocarbon observations, but instead of deriving the best-fit transfer velocity by region, we sought to directly estimate the global mean transfer velocity \bar{k} and the windspeed dependence exponent n that best fit ocean bomb radiocarbon observations. We simulated ocean bomb radiocarbon uptake for different values of n and \bar{k} on a mesh using a spacing of 0.3 in n and 0.1 times the *Wanninkhof* [1992] value (or about 2 cm / hour) in \bar{k} . We solved for the best-fit values by linearizing a misfit function, as in the first approach, about the combination of \bar{k} and n in our mesh that had the smallest misfit.

Ocean ^{14}C data

We compared our simulated bomb radiocarbon fields with a quality-controlled compilation of 17,501 measurements of radiocarbon in ocean water samples prepared by the Global Ocean Data Analysis Project (GLODAP) [Key *et al.*, 2004], which represent 1,070 depth profiles (Figure 3). The compilation includes measurements from GEOSECS in the 1970s and from several cruises in the 1980s, with a predominance of measurements from the WOCE program in the 1990s. As part of GLODAP, gridded maps of ocean total and bomb radiocarbon were also developed based on interpolation from WOCE-era measurements [Key *et al.*, 2004].

A measurement of an ocean sample taken in the 1970s-1990s reveals only its total $\Delta^{14}\text{C}$. To compare this measurement to a simulated value of bomb $\Delta^{14}\text{C}$ requires an estimate of the water's 1950s (pre-bomb) $\Delta^{14}\text{C}$, which can be then subtracted to yield the bomb enhancement. For most of the ocean $\Delta^{14}\text{C}$ measurements, GLODAP provides estimates of this background level and of the bomb enhancement component. These are based primarily on the assumption that the water's pre-bomb $\Delta^{14}\text{C}$ is linearly related to its potential alkalinity. Water with higher potential alkalinity has generally been in the deep ocean longer, and thus had lost ^{14}C to decay. This relationship was calibrated using 1950s coral and surface water samples, as well as later deep water samples that contain little bomb radiocarbon [Rubin and Key, 2002]. The typical error in deducing $\Delta^{14}\text{C}$ from potential alkalinity is found to be around 12‰ [Rubin and Key, 2002]. This is much worse than the analytical precision of the $\Delta^{14}\text{C}$ measurements, typically around 5‰ [Key *et al.*, 2002].

An alternative approach to estimating the $\Delta^{14}\text{C}$ background, with roughly the same accuracy, is based on the water silica content: water high in silica tends to have low background $\Delta^{14}\text{C}$ [Broecker *et al.*, 1985; Broecker *et al.*, 1995; Peacock, 2004]. We calculated bomb radiocarbon values using this method as well, employing silica measurements for the same water samples (also from the GLODAP compilation) and the relationship between silica and background $\Delta^{14}\text{C}$ derived by Peacock [2004]. As a check on the sensitivity of our fit to the bomb radiocarbon component separation, we used both these silica-based determinations of bomb $\Delta^{14}\text{C}$ and the GLODAP ones, which are based primarily on potential alkalinity.

Comparing simulation with observations

As a first step to determining which air-sea gas transfer velocity distribution yields the best fit with observed bomb radiocarbon levels, we compared our simulated global bomb radiocarbon ocean total and its latitudinal distribution for the mid-1970s and mid-1990s (at the middle of the GEOSECS and WOCE periods, respectively) with available observation-based inventories [Broecker *et al.*, 1995; Key *et al.*, 2004; Peacock, 2004]. To more rigorously determine the best-fit form of the air-sea gas transfer velocity, we compared bomb radiocarbon levels in individual measurements, or alternatively column inventories (the integrals of bomb radiocarbon depth profiles), with model-predicted levels for the same months and grid cells, using data from either the GEOSECS period (1970s) or the WOCE period (1980s-1990s). Many more measurements are available from the 1990s, but because much more time has passed since the period of

fastest ocean bomb radiocarbon uptake (~30 years as opposed to ~10 years in the 1970s), the effect of transport errors on attributing source regions to the observed radiocarbon distribution is likely to be larger. For our first approach (solving for the best-fit mean gas transfer velocity by region), we will show only results obtained using GEOSECS data, since WOCE measurements turned out to be unable to consistently distinguish between uptake in some pairs of adjacent regions.

For a given set of observations, we determined which regional gas transfer velocities, or which global mean and windspeed dependence of the gas transfer velocity, minimized the overall misfit between the observations and model predictions. This problem is one of minimizing some norm of the weighted deviation between two vectors representing observations and predictions respectively, so that the minimum-misfit parameter values can be expressed in the form

$$\mathbf{x}^* = \min_{\mathbf{x}} \|\mathbf{C}^{-1/2}(\mathbf{b} - \mathbf{A}(\mathbf{x}))\|^2, \quad (5)$$

where \mathbf{x} is a vector of the unknown parameters, \mathbf{b} is a vector of the observations, $\mathbf{A}(\mathbf{x})$ are the model predictions as a function of the unknown parameters, \mathbf{C} is a covariance matrix representing error in \mathbf{b} , and $\|\cdot\|$ denotes a norm, in this case of the weighted deviation between predictions and observations. Specifying \mathbf{C} for a comparison between measurements and an ocean model is challenging [e.g. Wunsch, 1996]. Sources of uncertainty for the comparison between observations and simulation include measurement error, error in estimating the bomb enhancement from the measured total $\Delta^{14}\text{C}$, interannual and small-scale variability in ocean transport not included in the model [Peacock *et al.*, 2005], and any number of spatially variable shortcomings in model transport. Here, we assumed that the error covariance matrix \mathbf{C} is diagonal, although in

fact the transport and bomb component attribution errors appear to show spatial autocorrelation, with the errors associated with observations that are close in space and time tending to be similar [cf. *Michalak et al.*, 2004 in an atmospheric inversion context]. For comparing individual measurements or column inventories, we assumed the error of each measurement or column inventory to be the same, meaning that all observations or column inventories were weighted equally.

In standard least-squares minimization, the vector 2-norm of the misfit is minimized in Equation 5; this minimum is easy to compute and is theoretically the maximum-likelihood estimate if the errors have a Gaussian distribution with the assumed covariance matrix \mathbf{C} . In our comparisons we found that there are often more extreme values in the modeled–measured residual than in a Gaussian distribution, as occasional unusually large modeled-measured misfits result from, for example, a bomb radiocarbon measurement made below the thermocline at a depth that in the model was above the thermocline and hence had a much higher predicted bomb radiocarbon content. Minimizing a 2-norm would lead to these outlying measurements unduly influencing the best-fit parameter values, so we have preferred to calculate minimum misfits using the 1-norm (the sum of the residual’s absolute values), which should be more reliable in the presence of outliers [e.g. *Aster et al.*, 2005, Section 2.4]. We estimated 1 standard deviation uncertainty ranges for the 1-norm minimum from the curvature of the misfit function near its minimum using the results of *Parker and McNutt* [1980] and approximating the misfit function as parabolic.

Atmospheric evidence for 1990s ocean ^{14}C uptake

For the WOCE period (centered around 1994), extensive ocean $\Delta^{14}\text{C}$ surface measurements were used by *Key et al.* [2004] to construct a sea-surface $\Delta^{14}\text{C}$ climatology. We used this climatology, along with Equation 4, to compute the expected latitudinal gradient in $\Delta^{14}\text{C}$ of atmospheric CO_2 for different windspeed dependences of air-sea gas exchange, without reference to an ocean circulation model. To do this, we had to account for other substantial contributors to the latitudinal gradient. We assumed that long-term cosmogenic production averages $6.2 \text{ kg }^{14}\text{C} / \text{year}$, balancing decay in short-term carbon pools [*Goslar, 2001*] and consistent with observed ^{14}CO concentrations [*Quay et al., 2000*], and that interannual variability in production is proportional to the sunspot number [*Lingenfelter, 1963*]. Carbon from fossil fuels contains no ^{14}C , and so the concentration of fossil fuel burning in the northern midlatitudes results in $\Delta^{14}\text{CO}_2$ depletion in the northern hemisphere [*Levin et al., 2003*]. We model this surface flux using distributions of fossil CO_2 emissions from *Andres et al.* [1996]. Also, most of the respired biomass in the 1990s was fixed when the atmosphere contained more bomb ^{14}C , with the result that since the 1980s, land biosphere respiration has been a net source of ^{14}C . This ^{14}C -enriched flux is highest in the tropics and in the north temperate zone where net primary production is high [*Randerson et al., 2002*]. We modeled this flux using spatially and seasonally resolved biomass respiration pulse functions derived from the CASA biosphere model [*Thompson and Randerson, 1999*] convolved with the atmospheric $\Delta^{14}\text{C}$ history.

There has been significant interannual variability in the rate of decline of the $\Delta^{14}\text{C}$ of atmospheric CO_2 [e.g. *Levin and Kromer, 2004*]. We estimate this rate of decline as

7.0±0.6‰ / year for a 5-year period centered around 1994 by taking the average of available long-term atmospheric $\Delta^{14}\text{C}$ measurement series (Table 1). We estimated the contributions of the major influences on the atmospheric $^{14}\text{CO}_2$ isotopic budget (Table 2) and calculated the dependence of the ocean uptake on the parameters \bar{k} and n . Uncertainty in several other contributions to the rate of decline was also around 0.6‰ / year (Table 2), and adding their contributions to the error variance yielded a total uncertainty of ±1.4‰ / year for the model-data comparison.

Published data on the latitudinal distribution of atmospheric $\Delta^{14}\text{C}$ in the 1990s are scarce. ^{14}C uptake in the Southern Ocean is the major influence on the $\Delta^{14}\text{C}$ gradient between the tropics and high southern latitudes, while $\Delta^{14}\text{C}$ gradients in the northern hemisphere are dominated by the influence of fossil carbon emissions [e.g. *Levin et al.*, 2003]. We compared the mean difference of 5.6±2.8‰ observed for 1993-1994 between Llano de Hato, Venezuela (9°N) and Macquarie Island in the Southern Ocean southeast of Australia (54°S) [*Levin and Hesshaimer*, 2000] to that predicted by our atmospheric transport model for different air-sea gas exchange parameter values after accounting for the effect of other exchange processes (Table 2). Uncertainty in the predicted gradient due to model transport is about the same size as the reported measurement error but varies depending on the absolute size of the predicted gradient; the total uncertainty for the model-data comparison was about 4.5‰ (Table 2).

Preindustrial ocean ^{14}C uptake

We modeled air-sea ^{14}C fluxes using Equation 3, an atmospheric $\Delta^{14}\text{C}$ level of 0‰, and the GLODAP climatology of estimated pre-bomb ocean surface $\Delta^{14}\text{C}$ [Key *et al.*, 2004], which we corrected by using the a simulation with MOM (run with the Wanninkhof [1992] air-sea gas transfer velocity) to estimate the small depletion attributable to pre-bomb fossil fuel dilution.

The total amount of ^{14}C in the preindustrial ocean can be determined to an accuracy of perhaps 2% by integrating the pre-bomb ^{14}C distribution estimated by GLODAP and making a small correction for the effect of fossil fuel CO_2 to 1956. To estimate the preindustrial air-sea ^{14}C flux, one could assume steady state and take the net flux into the ocean to match the decay of ^{14}C in ocean DIC; this amount is $5.4 \text{ kg } ^{14}\text{C}$ ($2.3 \times 10^{26} \text{ } ^{14}\text{C}$ atoms) per year. This assumption is open to question, however, since it fails to account for exchange of DIC with other carbon pools with low $\Delta^{14}\text{C}$, such as carbonate and organic sediment and volcanic or hydrothermal CO_2 ; the magnitude of this exchange is poorly known [Damon and Sternberg, 1989; Goslar, 2001]. For example, a plausible total input of 0.5 Pg per year of carbon containing essentially no ^{14}C would increase the steady-state air-sea flux required by $0.6 \text{ kg } ^{14}\text{C} / \text{year}$, or $\sim 11\%$. In addition, some deviation from steady state flux, caused for example by long-term oscillations in the atmospheric ^{14}C production rate [Lingenfelter, 1963] or in ocean circulation, is to be expected. Also allowing for uncertainty in the preindustrial ocean-surface $\Delta^{14}\text{C}$, we estimated the preindustrial air-sea flux at $5.4 \pm 1 \text{ kg } ^{14}\text{C} / \text{year}$ and compared it with that predicted for different values of \bar{k} and n .

The preindustrial interhemispheric $\Delta^{14}\text{C}$ gradient has been carefully measured (with replicate northern and southern samples analyzed in two laboratories to eliminate

intercalibration error) as the offset in cellulose $\Delta^{14}\text{C}$ between tree rings from Britain and New Zealand [Hogg *et al.*, 2002]. Some oscillation over decade to century periods was found, with a mean \pm standard deviation of $4.8\pm 1.6\text{‰}$ over the period 950-1850. (From earlier tree ring measurements, *Braziunas et al.* [1995] estimated a similar preindustrial gradient of $4.4\pm 0.5\text{‰}$ between the northern and southern midlatitudes.) We compared this gradient with that predicted by our atmospheric transport model to result from air-sea gas exchange for different values of \bar{k} and n . Based on the spread of TransCom models, we estimated the atmospheric transport uncertainty at $\pm 1.0\text{‰}$, for a total uncertainty of $\pm 1.9\text{‰}$ for the model-data comparison.

Air-sea ^{13}C exchange

We constructed an isotopic budget of ^{13}C in the atmosphere for around 1995 based on the observed rate of decline in $\delta^{13}\text{C}$ of atmospheric CO_2 together with estimates of fossil fuel emissions and biosphere and ocean exchanges and their isotopic composition (Table 3), using an estimate of the oceanic uptake of anthropogenic CO_2 based on ocean DIC measurements [Mikaloff Fletcher *et al.*, in press] to determine the relative magnitudes of land and ocean carbon uptake. This budget implies a disequilibrium air-sea ^{13}C isotope flux of $77\pm 16 \text{ Pg C } \text{‰} / \text{year}$ out of the ocean for the mid-1990s (Table 3), which agrees well with the estimate of $62\pm 32 \text{ Pg C } \text{‰} / \text{year}$ for a period centered in the 1980s derived by Quay *et al.* [2003] from observations of the decline in ocean $\delta^{13}\text{C}$ between the 1970s and 1990s. (Our simulation of ocean ^{13}C uptake suggests that the air-sea ^{13}C flux increased by some $14 \text{ Pg C } \text{‰} / \text{year}$ between the mid-

1980s and mid-1990s, further improving the agreement between our estimate and that of *Quay et al.* [2003].) If we account for a steady-state 8 ± 4 Pg C %_o / year flux into the ocean that balances the influx of ~ 0.4 Pg C / year of organic material depleted ~ 19 % relative to the atmosphere that enters as runoff [*Heimann and Maier-Reimer*, 1996; *Aumont et al.*, 2001] (Table 3), we arrive at a total air-sea ^{13}C flux of 70 ± 17 Pg C %_o / year. We compared this value with the flux predicted by estimates of the air-sea $\delta^{13}\text{C}$ disequilibrium based on surface ocean measurements, combined with different formulations for air-sea gas transfer.

Extensive, accurate measurements of the $\delta^{13}\text{C}$ of sea-surface DIC were made for the first time in the 1980s and 1990s as part of WOCE and related cruises [*Gruber et al.*, 1999; *Quay et al.*, 2003]. We interpolated the sea-surface $\delta^{13}\text{C}$ measurements in GLODAP (mostly taken 1991-1999; median year, 1995) and used latitudinally and seasonally varying values for the $\delta^{13}\text{C}$ of atmospheric CO_2 for the mid 1990s based on measurements from the Scripps [*Keeling et al.*, 1995] and NOAA/CMDL [*Trolier et al.*, 1996] networks together with isotopic fractionation factors for air-sea exchange from *Zhang et al.* [1995] to predict the ^{13}C isotope flux for different global mean air-sea gas transfer velocities \bar{k} and exponential dependences on windspeed n .

In comparing this predicted isotope flux with that inferred from the atmospheric record, additional uncertainties are introduced by possible error in the fractionation factors, by the interpolation of sea-surface $\delta^{13}\text{C}$, and by any intercalibration offset between the atmospheric and sea-surface $\delta^{13}\text{C}$ measurements. As a sensitivity test, we tried using the sea-surface $\delta^{13}\text{C}$ field of *Gruber and Keeling* [2001], based on different measurements and interpolation procedures, and found that the predicted global air-sea

isotope flux was within about 5 Pg C ‰ / year of that obtained by interpolating $\delta^{13}\text{C}$ measurements from GLODAP, suggesting that interpolation and calibration errors in the $\delta^{13}\text{C}$ fields are probably smaller than the uncertainty in inferring the air-sea ^{13}C flux from atmospheric and other observations, which is of order ± 17 Pg C ‰ / year (Table 3).

The latitudinal contrast in the direction of the ^{13}C isotope flux would have also existed in preindustrial times, and we can assume that, since the $\delta^{13}\text{C}$ of atmospheric CO_2 changed much more slowly, the net air-sea isotope flux was small. At steady state, we would expect only the aforementioned flux of 8 ± 4 Pg C ‰ / year into the ocean, which balanced incoming river carbon. The preindustrial sea-surface $\delta^{13}\text{C}$ can be estimated from the WOCE-era distribution by subtracting from it the impact of recent exchange with atmospheric CO_2 , whose $\delta^{13}\text{C}$ has been declining due to fossil emissions. We used a simulation with the MOM ocean transport fields, with the *Wanninkhof* [1992] air-sea gas exchange parameterization and a history of the decline in the $\delta^{13}\text{C}$ of atmospheric CO_2 since 1800 reconstructed from gas trapped in ice [*Francey et al.*, 1999], to estimate this perturbation in sea surface $\delta^{13}\text{C}$. To allow for error in the estimated perturbation, we increased the assumed uncertainty of the preindustrial flux to ± 10 Pg C ‰ / year for the purpose of comparing it with the predicted flux under different air-sea gas exchange scenarios.

Results: ocean bomb ^{14}C

Total amount of ocean bomb ^{14}C

The total ocean bomb radiocarbon uptake simulated using our ocean model depends primarily on the global mean transfer velocity \bar{k} (Figure 5). Increasing \bar{k} by 1% increases the simulated GEOSECS-era inventory by around 0.8% and the WOCE-era inventory by around 0.5%. Especially for the later (WOCE) period, modeled uptake is also slightly greater at high n , since this shifts uptake in high latitudes, where more deep water reaches the surface over a given period than at low latitudes so that the exchange-weighted air-sea disequilibrium term ($\Delta_{\text{sea}}^{14}\text{C} - \Delta_{\text{air}}^{14}\text{C}$) in Equation 4 is more negative.

When \bar{k} is equal to the *Wanninkhof*[1992] value of 20.6 cm / hour, our model ocean total is $293\text{-}309 \times 10^{26}$ atoms for the beginning of 1975 and $348\text{-}382 \times 10^{26}$ atoms for mid-1994, depending on n (Figure 5). This amount is broadly consistent with previous data-based estimates [*Broecker et al.*, 1995; *Key et al.*, 2004; *Peacock*, 2004]. On the grid we used, the GLODAP mapping of WOCE observations (mostly using potential alkalinity to separate the bomb component) sums to 322×10^{26} atoms of bomb radiocarbon (3% higher than the 313×10^{26} atoms reported by *Key et al.* [2004]). This mapping excludes the Arctic Ocean and some marginal seas. Using our model concentration field for 1994 to extrapolate to the entire ocean adds an additional 13% for a WOCE-era total ocean amount of 364×10^{26} atoms (shown in Figure 5b). *Key et al.* [2004] estimate the uncertainty on the total amount at 15%, or $\pm 55 \times 10^{26}$ atoms. With this uncertainty, the WOCE inventory implies a value of \bar{k} in the range of 15-31 cm / hour (Figure 5b). This broad range is compatible with either the *Broecker et al.* [1995] estimate of $305 \pm 30 \times 10^{26}$ atoms or the *Peacock* [2004] estimate of some $270 \pm 25 \times 10^{26}$ atoms for the global GEOSECS-era ocean total, which imply values of \bar{k} in the range of 18-24 or 15-20 cm / hour, respectively (Figure 5a).

The correlation between the bomb radiocarbon levels inferred from GLODAP ocean measurements and the modeled levels at the same time and space when \bar{k} and n were close to the *Wanninkhof*[1992] values was +0.93, using either the potential alkalinity or the silica method to estimate the bomb radiocarbon component of the GLODAP observations. (This is higher than the corresponding correlation with CFC measurements, possibly because the slow air-sea exchange of ^{14}C as compared with CFCs makes its distribution less sensitive to seasonality in ocean transport patterns, which is not represented by our pulse functions.) At the *Wanninkhof*[1992] reference global mean gas transfer velocity \bar{k} (20.6 cm / hour), our model reproduced fairly well the latitudinal structure estimated from measurements both for the GEOSECS period [*Broecker et al.*, 1995; *Peacock*, 2004] and for the WOCE period [*Key et al.*, 2004]. The amount of bomb ^{14}C in the Southern Ocean was better simulated if we assumed a linear or no dependence of the transfer velocity on windspeed (Figure 6).

While the global total is relatively insensitive to the windspeed dependence n of the gas transfer velocity, Figure 6 suggests that the simulated latitudinal distribution of bomb radiocarbon is sensitive to n . The following approaches exploit observations of the regional distribution of bomb radiocarbon to estimate concurrently both \bar{k} and n .

Estimates of the mean gas transfer velocity by region

Figure 7 shows the regional mean gas transfer velocities estimated from GEOSECS ocean radiocarbon measurements, compared with the values implied by the *Wanninkhof*[1992] parameterization. Figure 8 compares these estimated regional rates

with those predicted using commonly-used published parameterizations of the gas transfer velocity as a function of windspeed, shown as solid curves. The range of gas transfer velocities we estimated is somewhat higher than that implied by the *Wanninkhof* [1992] parameterization in the north subtropical, equatorial, and south subtropical Atlantic and in the eastern Equatorial Pacific, and somewhat lower in the north Pacific. We estimated the transfer velocity in the Southern Ocean (south of 45° S) at 21-30 cm / hour, considerably lower than the prediction of 38 cm / hour given by the *Wanninkhof* [1992] parameterization. Overall, a weak relationship with regional windspeed is evident (Figure 8), consistent with a roughly linear dependence of the gas transfer velocity on windspeed. Specifically, the best-fit power law relationship between regional root mean square windspeed and the estimated regional transfer velocities – derived by minimizing the 1-norm misfit, with the uncertainty for each of the estimated transfer velocities taken to be the range shown in Figure 7 (the gray vertical bars in Figure 8) – has an exponent n of 1.11 ± 0.37 and a global mean \bar{k} of 20.6 ± 0.6 cm / hour (black dashed curve in Figure 8). This relationship implies typically higher gas transfer velocities at low windspeeds and lower rates at high windspeeds than the *Wanninkhof* [1992] quadratic or *Wanninkhof and McGillis* [1999] cubic dependence, but essentially the same global mean transfer velocity, and higher transfer velocities at all windspeeds compared with the *Liss and Merlivat* [1986] and *Nightingale et al.* [2000] relationships, which yield lower global mean transfer velocities (Figure 8).

Global parameterization of gas exchange as a function of windspeed

Figure 9 shows the optimum values of the global mean gas transfer velocity \bar{k} and the windspeed dependence exponent n (Equation 3) obtained by minimizing the misfit of modeled with measured bomb ^{14}C . Figure 9a shows the optimum values for \bar{k} and n estimated by fitting individual ocean GEOSECS (1970s) bomb ^{14}C measurements or their column integrals; Figure 9b show the corresponding results when 1980s-1990s (mostly WOCE) data were used. In each panel, the letter A and the contour lines show the minimum misfit obtained using the individual measurements and the GLODAP bomb component estimate (based on potential alkalinity); B shows the minimum misfit for individual measurements and a bomb component estimate based on silica; and C and D show the minimum misfit obtained using column integrals and, respectively, potential alkalinity or silica-based estimates of the bomb component. The posterior uncertainties, assuming that the each measurement is independent, were small – for example, about 0.25 cm / hour for \bar{k} and 0.06 for n when using individual GEOSECS measurements – compared with the variability in the misfit minimum location between the cases. It is likely that much of the error is highly correlated between individual measurements, so that our assumption of uncorrelated errors greatly underestimates the actual error (overestimates the effective number of data degrees of freedom).

Across all cases, we found the best-fit windspeed dependence of the gas transfer velocity to be consistently less than quadratic, with the exponent n ranging from below zero (which would mean that regions with low mean windspeed tend to have high gas transfer velocities) to about 1, while \bar{k} ranged from 17 to 25 cm / hour. With no obvious cause to believe that any of the cases we tried yields more reliable results than the others, we took the mean and standard deviation of the minimum-misfit \bar{k} and n values across

the cases shown in Figure 9 (first setting any negative values for the optimum n to 0) to obtain $n = 0.61 \pm 0.40$ and $\bar{k} = 20.7 \pm 2.4$ cm / hour. We then averaged these values of \bar{k} and n with those obtained by first estimating the transfer velocity for each region (see previous section), but retained the larger of the two approaches' standard deviations to allow for systematic error in either of them. This gave $\bar{k} = 21 \pm 2$ cm / hour and $n = 0.9 \pm 0.4$ as the parameters in a power-law relationship of gas transfer velocity with windspeed (Equation 3) that best reproduce the observed ocean distribution of bomb carbon-14. We turn to other carbon-14 and carbon-13 observations to determine whether these results are robust – in particular, whether our finding that $n < 2$ holds up.

Results: other ^{14}C and ^{13}C observations

1990s air-sea ^{14}C exchange

Our fit for the dependence of the gas transfer velocity on windspeed to ocean bomb radiocarbon observations (taking $\bar{k} = 21$ cm / hour and $n = 0.9$) yielded a predicted atmospheric $\Delta^{14}\text{C}$ decline rate of 7.7‰ / year, while the predicted decline rate was 8.7‰ / year assuming the *Wanninkhof* [1992] quadratic dependence on windspeed, and 9.7‰ / year assuming the cubic dependence of *Wanninkhof and McGillis* [1999] (Figure 10a). The observed decline rate together with our estimate of the combined measurement uncertainty and uncertainties in the other influences (Table 1) of 7.0 ± 1.4 ‰ / year implies that if we assume that \bar{k} is 21 cm / hour, then n is around 0.3. The 1- σ range given the estimated uncertainty of 1.4‰ is 0-1.6, meaning that a quadratic or cubic dependence on

windspeed yields too fast an atmospheric $\Delta^{14}\text{C}$ decline rate. If we assume that $n = 0.9$, \bar{k} is 19 ± 4 cm / hour.

At the *Wanninkhof* [1992] value for \bar{k} , the predicted Venezuela-Southern Ocean gradient was 4.2‰ for our parameterization of the dependence of the gas transfer velocity on windspeed, 7.5‰ assuming a quadratic dependence, and 10.8‰ assuming a cubic dependence (Figure 10b). The measured gradient of 5.6 ± 4.5 ‰, suggests that n is around 1.3 (range: 0-2.7) if we assume that \bar{k} is 21 cm / hour. If we assume that $n = 0.9$, the latitudinal gradient suggest that \bar{k} is 24 ± 11 cm / hour.

In our simulations using an atmospheric model, the windspeed dependence of the gas exchange transfer velocity was predicted to have a dominant effect on the latitudinal variation in atmospheric $\Delta^{14}\text{C}$ in the southern hemisphere (Figure 11). Accurate measurements and models may be able to use this latitudinal variation to determine the mean transfer velocity in the Southern Ocean independently of ocean-interior ^{14}C .

Preindustrial air-sea ^{14}C exchange

The dependence of the ocean uptake estimated from the sea-surface $\Delta^{14}\text{C}$ distribution on n was weak: the predicted air-sea flux was 5.5 kg ^{14}C / year for our parameterization for the dependence of the gas transfer velocity on windspeed ($n=0.9$), 5.8 assuming a quadratic dependence ($n=2$, as in *Wanninkhof* [1992]), and 6.2 assuming a cubic dependence ($n=3$, as in *Wanninkhof and McGillis* [1999]). Pending more detailed knowledge of preindustrial ^{14}C flows in the oceans, these all seem plausible. Conversely, as long recognized [*Craig*, 1957; *Broecker and Peng*, 1982, Chapter 3], the preindustrial

^{14}C steady state does fix the global mean transfer velocity \bar{k} to within $\sim 25\%$, supporting the range we and earlier workers derived from ocean bomb ^{14}C measurements.

Specifically, if we assume that the windspeed dependence exponent n is 0.9, \bar{k} must be 21 ± 4 cm / hour for the air-sea flux to have been in the range of 5.4 ± 1 kg / year.

We also compared the observed preindustrial Britain-New Zealand gradient in atmospheric $\Delta^{14}\text{C}$ of $4.8 \pm 1.6\text{‰}$ with that predicted by our atmospheric transport model for different values of \bar{k} and n (Figure 10d). The predicted gradient was 4.6‰ for our parameterization of the dependence of the gas transfer velocity on windspeed, 5.9‰ assuming the *Wanninkhof* [1992] quadratic dependence, and 7.2‰ assuming the *Wanninkhof and McGillis* [1999] cubic dependence. If we assume a global mean velocity \bar{k} of 21 cm / hour, the observed gradient of 4.8‰ suggests that n is around 1.1 (range: 0-2.5); if we assume that the windspeed dependence exponent n is 0.9, the observed gradient suggests that \bar{k} is 22 ± 9 cm / hour.

The air-sea ^{13}C isotope flux

The air-sea ^{13}C isotope flux only weakly constraints the mean gas transfer velocity (Figure 12a). However, it provides strong support for a low windspeed exponent. The predicted 1990s fluxes were 58 Pg C ‰ / year for our gas exchange parameterization, 37 Pg C ‰ / year for the *Wanninkhof* [1992] quadratic dependence on windspeed, and 19 Pg C ‰ / year for the *Wanninkhof and McGillis* [1999] cubic dependence. Comparing the predicted isotope fluxes with that estimated from the atmospheric ^{13}C budget (Table 3) suggested that the windspeed dependence exponent n is

low (Figure 12a). If $\bar{k} = 21$ cm / hour, n must be around 0.1 (range: 0-1.2) for the isotope flux to 70 ± 17 Pg C ‰ / year as inferred from observations.

In the reconstructed preindustrial case, a steady state assumption also implied a relatively low dependence on windspeed (Figure 12b). The predicted fluxes (with the negative sign denoting an isotope flux of ^{13}C into the ocean) were -5 Pg C ‰ / year for our gas exchange parameterization, -19 Pg C ‰ / year for the *Wanninkhof* [1992] quadratic dependence on windspeed, and -34 Pg C ‰ / year for the *Wanninkhof and McGillis* [1999] cubic dependence. Again, if $\bar{k} = 21$ cm / hour, n must be around 1.1 (range: 0.3-1.9) for the isotope flux to be within the range of -8 ± 10 Pg C ‰ / year implied under a steady-state assumption.

Discussion

The air-sea gas transfer velocity: comparison with previous results

Our comparison of modeled with measured ocean bomb radiocarbon distributions, whether we solve for mean transfer velocity by region or solve for a best-fit exponential relationship with windspeed, suggests that globally, long-term mean gas exchange increase roughly linearly with root-mean-square windspeed ($n = 0.9 \pm 0.4$), and that latitudinal gradients in the gas transfer velocity are smaller than a quadratic or, especially, a cubic dependence on windspeed would imply. The requirement of an approximate preindustrial steady state constrains the global mean transfer velocity \bar{k} (Figure 10c), and

yields values that cover the range we obtained from ocean bomb radiocarbon data. The preindustrial latitudinal gradient, as well as 1990s ocean surface and atmospheric measurements, are also sensitive to the windspeed dependence exponent n (Figure 10abd), although measurement and other uncertainties meant that some of the data we considered are consistent with a wide range in n . The observed decline rate of atmospheric $\Delta^{14}\text{C}$, as well as the requirement that the air-sea ^{13}C isotope flux estimated from sea-surface $\delta^{13}\text{C}$ measurements be consistent with the recent atmospheric $\delta^{13}\text{C}$ history and with an approximate preindustrial steady-state (Figure 12), constrain n to be less than 2, which agrees with the range we estimate from ocean bomb radiocarbon data. Table 4 lists the values for \bar{k} and n estimated from the various approaches we have presented. Our estimate of the global mean air-sea gas transfer velocity for ice-free water at a Schmidt number of $660 - 21 \pm 2$ cm / hour – matches well with earlier estimates based on ocean bomb radiocarbon [Broecker *et al.*, 1985], natural radiocarbon [Broecker and Peng, 1982], and radon-222 [Peng *et al.*, 1979].

If we take $\bar{k} = 21 \pm 2$ cm / hour and $n = 0.9 \pm 0.4$, our ocean transport simulations suggest that the total amount of bomb radiocarbon in the ocean was some $305 \pm 24 \times 10^{26}$ atoms at the beginning of 1975 (very similar to the estimate of Broecker *et al.* [1995] and somewhat higher than that of Peacock [2004]) and $368 \pm 21 \times 10^{26}$ atoms at the middle of 1994 (very similar to the estimate of Key *et al.* [2004] when adjusted for the ocean volume excluded from their inventory). We found no indication from observations of ocean bomb or natural radiocarbon uptake that the global mean air-sea gas transfer velocity is much lower than the original estimates based on GEOSECS, as Hesshaimer *et al.* [1994] argue.

Some earlier studies support our result of a relatively weak latitudinal variation in the mean air-sea gas transfer velocity. These include the radon-222 profiles evaluated by *Peng et al.* [1979], reflecting gas transfer velocity averaged over a few days, which showed little effect of windspeed and a fairly weak latitudinal gradient, and the study of preindustrial ^{14}C by *Braziunas et al.* [1995], which found it necessary to revise the mean air-sea transfer velocity in the Southern Ocean (south of 50°S) down to ~ 31 cm / hour to account for the relatively small north-south $\Delta^{14}\text{C}$ gradient found in tree rings. A low dependence of the gas transfer velocity on windspeed was also found to be most consistent with preindustrial steady-state for the air-sea ^{13}C isotope flux in an analysis by *Heimann and Monfray* [1989] based on sparse GEOSECS measurements of sea-surface $\delta^{13}\text{C}$.

The formulations for quadratic or cubic dependence of gas transfer on windspeed proposed by *Wanninkhof* [1992] and *Wanninkhof and McGillis* [1999] respectively were largely based on field studies that used tracer release experiments or eddy covariance measurements of gas fluxes to evaluate the dependence of gas exchange on windspeed, typically over a few days to weeks. Extrapolating from the results of a few measurement campaigns to a relationship with windspeed suitable for use globally is inherently very uncertain, though. Direct measurement of air-sea gas fluxes is difficult and is subject to a number of sources of potential and systematic error, despite recent technical improvements [e.g. *Fairall et al.*, 2000]. As well, the apparent dependence of gas exchange on a variety of factors not directly tied to windspeed, including surfactants, rain, and wave height [*Frost and Upstill-Goddard*, 1999; *Woolf*, 2005], means that the gas transfer velocity at a given windspeed could vary considerably between places and

seasons depending on these other conditions. This is particularly true for extrapolations of the transfer velocity to high windspeed, where theory and laboratory evidence suggest that the gas transfer velocity saturates under some conditions [Komori *et al.*, 1993; Donelan *et al.*, 2004]. As an example of the influence of factors other than windspeed, McGillis *et al.* [2004] found that the gas transfer velocity inferred from CO₂ eddy covariance in the eastern equatorial Pacific varied little with windspeed but was strongly affected by temperature gradients in the ocean mixed layer, which promoted surface turbulence.

Our technique of deducing a parameterization of the gas transfer velocity from observations of large-scale air-sea carbon isotope exchanges implicitly averages across this variability, resulting in a parameterization that represents regional-scale gas exchange over timescales of months to decades. Accurate long-term direct measurements of gas exchange at many representative sites would greatly improve understanding of the relative importance of different factors in governing variability in air-sea exchange across seasons and ocean regions and help suggest better parameterizations based on windspeed or other surface properties that can be determined remotely.

A recent review of field and laboratory measurements of the gas transfer velocity over a wide range of windspeeds [Zhao *et al.*, 2003] found an overall power law exponent of 1.35, only slightly higher than our result of 0.9 ± 0.4 . Zhao *et al.* also propose that the gas transfer velocity is better correlated with whitecap coverage than with windspeed. This would be because whitecap coverage reflects both windspeed and other factors that influence the gas transfer velocity, such as the presence of organic surfactant films that inhibit turbulence and the degree to which waves are fully developed at the

given wind stress (which depends on the consistency of the wind direction and the distance from shore). It would be worth examining whether a parameterization based on whitecap coverage would better account for the regional variability we found in the mean gas transfer velocity, compared with a parameterization based only of windspeed.

Whitecap coverage can be remotely determined using satellite instrumentation similar to that used for sensing windspeed [Monahan, 2002]. Sea-surface mean square slope is another quantity that can be sensed remotely from microwave backscatter measurements and has been suggested to predict the gas transfer velocity better than windspeed [Frew *et al.*, 2004; Turney *et al.*, 2005].

Implications for air-sea CO₂ fluxes

We examined the effect of air-sea gas exchange parameterizations on the air-sea CO₂ flux implied by the air-sea *p*CO₂ difference climatology compiled by Takahashi *et al.* [2002] for a nominal year of 1995 (Figure 13). The total uptake is sensitive to n as well as \bar{k} , since the tropical oceans, with low mean windspeeds, tend to release CO₂ while the high-latitude oceans, with higher mean windspeeds, tend to take it up. With this surface *p*CO₂ climatology, the predicted anthropogenic uptake is 1.8 Pg C / year using our parameterization of the gas transfer velocity dependence on windspeed, 2.5 Pg C / year using the Wanninkhof [1992] quadratic dependence, and 3.0 Pg C / year assuming the Wanninkhof and McGillis [1999] cubic dependence (Figure 13a). The uncertainty in ocean CO₂ uptake estimated using this method is large, because small adjustments to sea-surface *p*CO₂ due to, for example, the skin temperature correction for evaporative cooling

[*Van Scoy et al.*, 1995; *Ward et al.*, 2004] and respiration by microorganisms in the surface microlayer [*Garabetian*, 1991], as well as to errors induced by lack of sampling in some seasons and regions, have a large impact on the inferred global uptake. Independent observational estimates of anthropogenic ocean CO₂ uptake include 2.2±0.3 Pg C / year for around 1995 based on the C* method for estimating the anthropogenic enhancement of ocean DIC combined with several ocean circulation models [*Mikaloff Fletcher et al.*, in press], 2.0±0.4 Pg C / year for the 1990s based on water ages inferred from ocean CFC measurements [*McNeil et al.*, 2003], and 2.4±0.7 Pg C / year for the 1990s based on atmospheric oxygen measurements [*Plattner et al.*, 2002].

Figure 13b shows the CO₂ flux by latitude estimated from the *Takahashi et al.* [2002] pCO₂ climatology using our gas transfer velocity parameterization compared with quadratic and cubic dependences on windspeed. Our lower windspeed dependence implies less CO₂ uptake in the Southern Ocean and shifts the maximum uptake there north by several degrees, which resolves part of the discrepancy between the high Southern Ocean CO₂ uptake implied by this pCO₂ climatology and a quadratic or cubic dependence of gas exchange on windspeed and the low Southern Ocean CO₂ uptake inferred from the stable atmospheric CO₂ concentrations measured when going across the Southern Ocean [*Roy et al.*, 2003]. The regional distribution of the ocean CO₂ uptake implied by a quadratic dependence on windspeed is used as a prior constraint in many inversions for regional CO₂ fluxes that are based on atmospheric CO₂ measurements [e.g. *Gurney et al.*, 2003], so adopting a different dependence on windspeed could also affect the regional CO₂ sources and sinks inferred from such inversions. For example, the network of CO₂ observation stations does not distinguish land from ocean carbon sources

and sinks in the tropics, so this assignment depends on the use of other information, such as the distribution of the air-sea CO₂ flux [e.g. *Krakauer et al.*, 2004]. If CO₂ outgassing from the equatorial ocean is more intense than previously assumed, a smaller tropical land source might be required to explain the observed patterns in atmospheric CO₂ concentration.

Our higher estimate for the gas transfer velocity in the eastern equatorial Pacific highlights the potential significance of *p*CO₂ variations there with ENSO [*Feely et al.*, 1999; *Feely et al.*, 2004b] for interannual variability in ocean CO₂ uptake. Conversely, a smaller dependence of gas exchange on windspeed makes it less likely that changes in storm frequencies are a major contributor to interannual variability in the ocean sink [*Bates*, 2002; *Perrie et al.*, 2004].

Estimating gas transfer velocities from carbon isotope distributions: limitations and directions for improvement

Our analysis attempted to find the power law relationship of the gas transfer velocity with a particular satellite-based windspeed climatology that best fit a variety of atmosphere and ocean carbon isotope observations. This wind climatology could be supplemented with other satellite products to investigate whether using different wind climatologies makes any difference for the best-fit parameterization of gas transfer velocity, and the possible impact of interannual variability in winds could be checked using satellite products as well as reanalysis wind fields.

Given our finding of an approximately linear relationship of the gas transfer velocity to windspeed, it may be better to use, for example, arithmetic mean windspeed instead of the root-mean-square we used, which is best if the relationship of gas transfer velocity to windspeed is close to quadratic [cf. *Wanninkhof et al.*, 2004; *Olsen et al.*, 2005 for discussions of the impact of using different wind products and moments]. Also, a more complex function for the dependence of the gas transfer velocity on windspeed, in which, for example, the transfer velocity levels off at low windspeeds and plateaus at high windspeeds, may well better represent the variability in the transfer velocity over a variety of time and space scales than the simple power law relationship that we assumed.

Some of the data sets that we used to calculate the air-sea bomb radiocarbon flux could be improved. The zonal distribution of atmospheric $\Delta^{14}\text{C}$ in the 1960s, when gradients were very large, should be revisited in light of expanded tropical tree ring measurements [*Hua et al.*, 1999; *Hua and Barbetti*, 2004].

Judging by the differences we found between methods based on potential alkalinity and on silica for estimating the pre-bomb ocean $\Delta^{14}\text{C}$ distribution, which is used to determine the bomb ^{14}C component in post-bomb $\Delta^{14}\text{C}$ measurements, the pre-bomb $\Delta^{14}\text{C}$ distribution is a significant source of uncertainty. This is particularly important for the Southern Ocean, where because of more extensive mixing the absolute bomb $\Delta^{14}\text{C}$ enhancements tend to be smaller and thus harder to quantify, and where few early $\Delta^{14}\text{C}$ measurements were made [*Broecker et al.*, 1960]. Measurements of $\Delta^{14}\text{C}$ in banded ahermatypic corals [*Goldstein et al.*, 2001; *Frank et al.*, 2004], which grow in cold water, could help calibrate the pre-bomb $\Delta^{14}\text{C}$ profile in the Southern Ocean. Coral $\Delta^{14}\text{C}$ timeseries in general provide unique chronologies of bomb radiocarbon arrival, and

could supplement single measurements of water $\Delta^{14}\text{C}$ such as the ones in GLODAP as evidence for air-sea gas transfer velocity.

Another uncertainty in our ocean bomb ^{14}C results comes from our ocean transport model. While our model appears to represent the global inventory and latitudinal distribution of tracers such as CFCs and bomb ^{14}C quite accurately over decadal timescales, it is harder to validate its skill in assigning uptake to smaller regions, especially given the low resolution imparted by using regional pulse functions. Intercomparison of bomb radiocarbon distribution dependence on air-sea transfer velocity over different transport models, similar to the OCMIP-3 project of solving for best-fit air-sea CO_2 fluxes from different models [*Mikaloff Fletcher et al.*, in press], would at least permit better assessment of the magnitude of transport error. Ultimately, a fully inverse approach, where ocean circulation fields and the distribution of the mean air-sea gas transfer velocity are estimated simultaneously using measurements of bomb ^{14}C together with other ocean tracers [cf. *Schlitzer*, 2000] within an ocean data assimilation framework such as ECCO, is likely to be the most effective way to utilize the large number of available ocean $\Delta^{14}\text{C}$ measurements to infer detailed spatial patterns in gas transfer velocity.

We have shown that the 1990s rate of decline in and latitudinal profile of the $\Delta^{14}\text{C}$ of atmospheric CO_2 reflect the latitudinal distribution of the air-sea gas transfer velocity. Continued measurement of atmospheric $\Delta^{14}\text{C}$ and of sea-surface $\Delta^{14}\text{C}$ in the Southern Ocean would therefore provide information about the mean rate of air-sea gas exchange in the Southern Ocean averaged over the atmospheric transport timescale (a few months), and in principle could even detect seasonal and interannual variability in the Southern

Ocean transfer velocity, although the precision requirement is high. Given the importance of Southern Ocean gas exchange to climate and to CO₂ uptake [Liss *et al.*, 2004], a long-term measurement program should be encouraged.

We have also shown that the ongoing air-sea isotopic flux of ¹³C, as well as the preindustrial flux, provides information about the windspeed dependence of the gas transfer velocity if the spatial distribution of the air-sea δ¹³C disequilibrium is well known. Further work is needed to find the best way of estimating this distribution from available measurements, possibly replacing the simple interpolation that we used with a more sophisticated approach using ocean transport models to map ocean surface δ¹³C in a way consistent with measurements, and to more fully assess the uncertainties in δ¹³C measurements and in the equilibrium air-sea isotopic fractionation.

Conclusions

The air-sea gas transfer velocity is important for quantifying the ocean gas exchange, and both field measurements and indirect inference from tracer distributions can help in developing a consistent formulation for it. We have estimated the mean gas transfer velocity both by region and as a function of climatological monthly windspeed from ocean bomb carbon-14 measurements as well as from other carbon-14 and carbon-13 data. Although many of the approaches we used yield substantial uncertainties, our results support a roughly linear increase of gas transfer velocity with windspeed in the global ocean (best-fit exponent: 0.9±0.4; global mean rate: 21±2 cm / hour at a Schmidt number of 660).

To account for model transport error, we recommend either comparing carbon-14 distributions for multiple models or else solving for transport simultaneously with air-sea exchange. High-precision measurement of atmospheric carbon-14 may be able to provide independent information on air-sea exchange, especially for the Southern Ocean.

Acknowledgements

We thank Gordon Brailsford and Stephan Woodbourne for sharing unpublished atmospheric radiocarbon measurements, Sara Mikaloff Fletcher for providing a preprint of her ocean carbon inversion manuscript, and Martin Heimann for informing us about his previous work on the dependence of the air-sea carbon-13 isotope flux on the variability of the gas transfer velocity between high and low latitudes. Seth Olsen provided the pulse functions that we used to model the effect of ocean uptake on atmospheric radiocarbon gradients. Jess Adkins and Tapio Schneider critically reviewed drafts of this paper. Discussions with Manuel Gloor, Andy Jacobson, Fortunat Joos, Robert Korty, Ernst Maier-Reimer, John Miller, Tobias Naegler, John Southon, Colm Sweeney, and Sue Trumbore valuably informed our perspectives on air-sea gas exchange and its consequences for carbon isotope budgets. NYK was supported by a graduate fellowship from the Betty and Gordon Moore Foundation and by a NASA Earth System Science graduate fellowship. This work was supported by NSF grants to JTR and Trumbore (EAR 0402062, 0223514, 0223157). NG acknowledges support from NASA. Many of the computations reported here were carried out on the University of California at Irvine's Earth System Modeling Facility (ESMF), which is funded by NSF grant ATM-0321380.

Figures

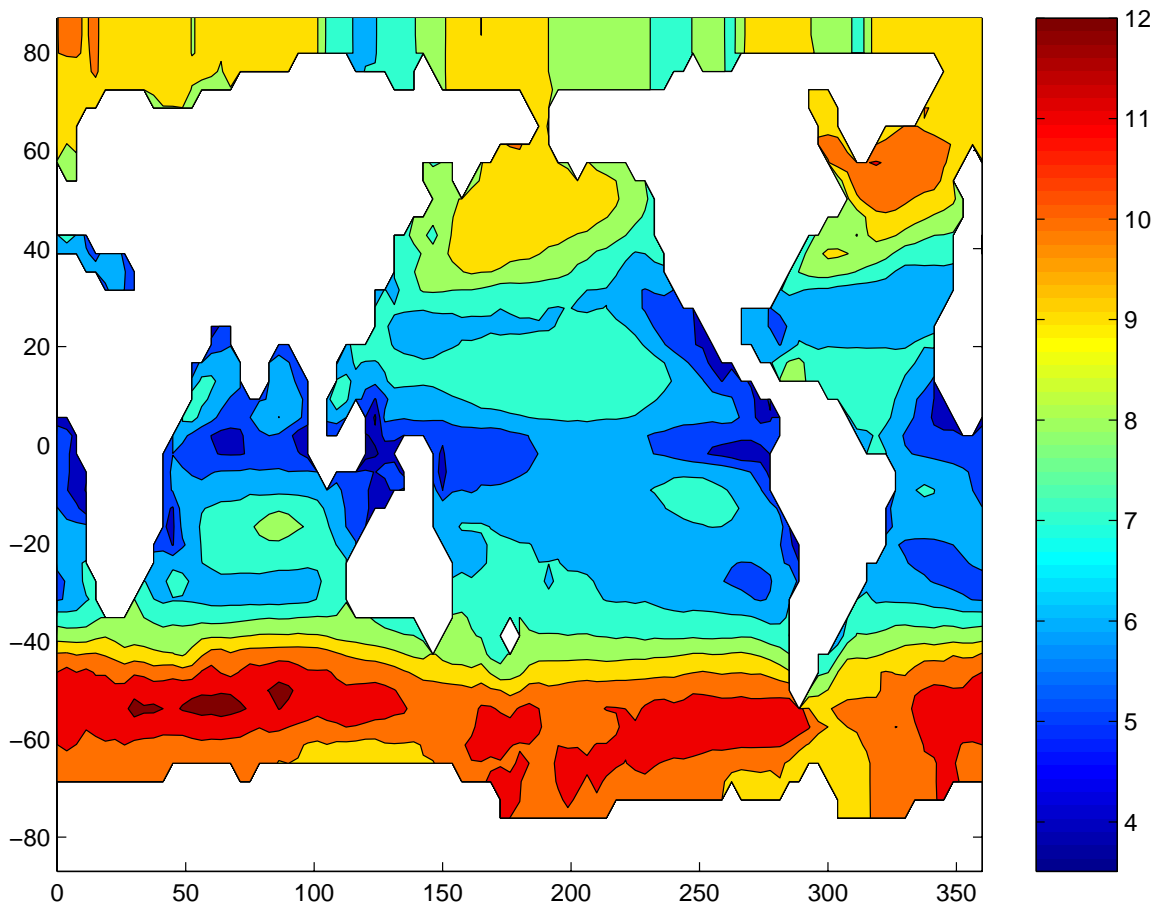


Figure 1. Annual-mean root-mean-square windspeed (m/s) over the ocean, at 10 m height, from the monthly climatology of *Boutin and Etcheto* [1997; *Orr et al.*, 2001], derived from satellite (SSM/I) data. We used the monthly climatology to explore the consequences of different dependences of the air-sea gas transfer velocity on windspeed on ocean carbon-14 uptake. The RMS windspeed varies from 5-6 m/s near the equator to around 11 m/s in the Southern Ocean.

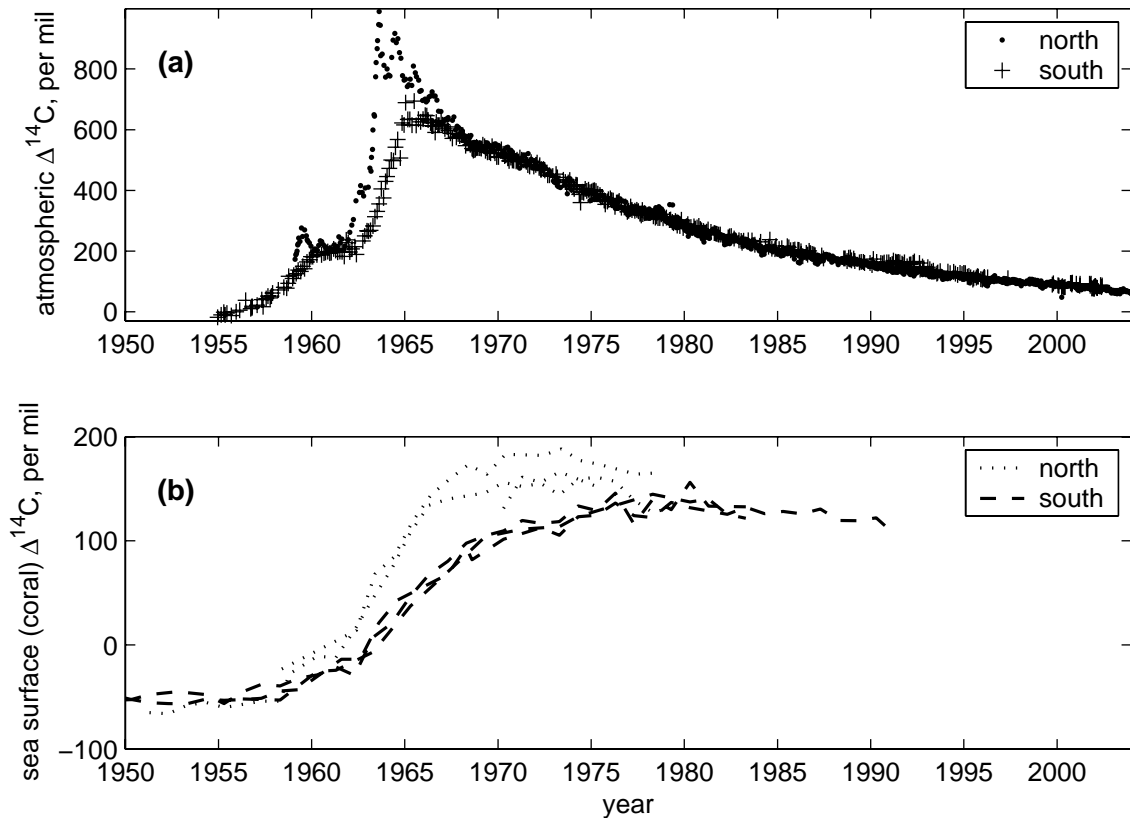


Figure 2. Representative northern and southern hemisphere observational timeseries of $\Delta^{14}\text{C}$ for CO_2 in air and for DIC in the upper ocean, showing the bomb radiocarbon spike. (a) Measurements of $\Delta^{14}\text{C}$ in atmospheric CO_2 in central Europe ($46^\circ\text{-}48^\circ\text{N}$) [Levin and Kromer, 2004] and in New Zealand (41°S) [G. Brailsford, personal communication, updating Manning *et al.*, 1990], at approximately fortnightly resolution. (b) Measurements of $\Delta^{14}\text{C}$ in subtropical ($20^\circ\text{-}25^\circ\text{N}$ and S) surface coral, at approximately annual resolution. The northern corals are from Florida [Druffel, 1989] and Oahu and French Frigate Reef in Hawaii [Druffel, 1987]. The southern corals are from Abraham Reef, Heron Island, and Lady Musgrave Island, all in the Great Barrier Reef off Australia [Druffel and Griffin, 1995].

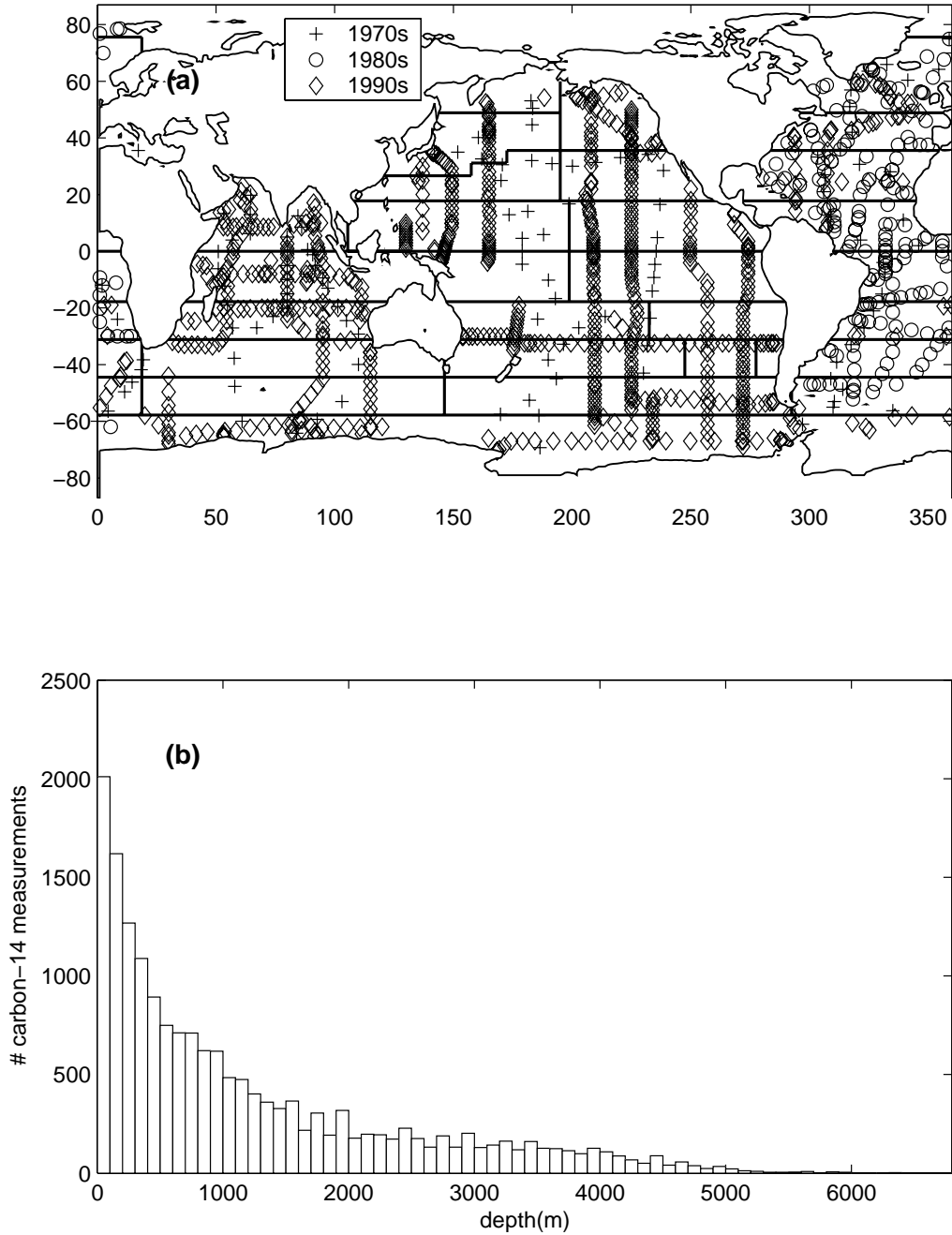


Figure 3. Distribution of the ocean radiocarbon measurements used in this analysis [Key *et al.*, 2004]. (a) Location of measurements, grouped by decade. The 1970s measurements were made as part of GEOSECS, the 1990s measurements mostly as part of WOCE. The thick lines are the boundaries between the 30 ocean regions we use as basis regions for transport pulse functions. (b) Depth distribution of measurements (100-m bins).

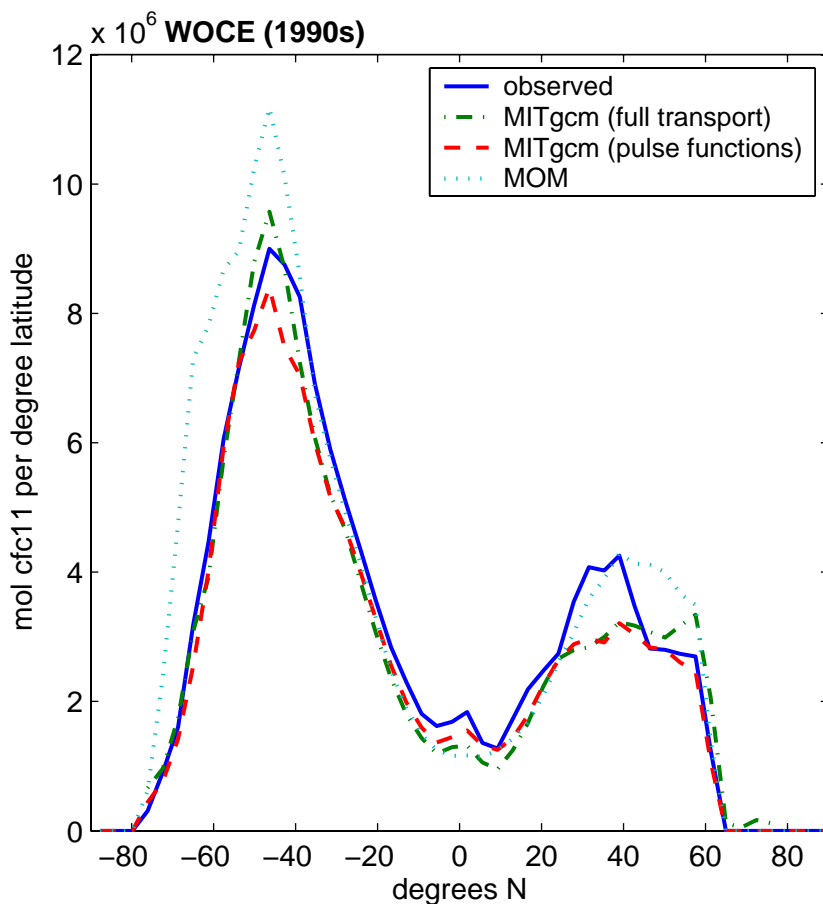


Figure 4. Modeled 1994 latitudinal distribution of the chlorofluorocarbon CFC-11 with the OCMIP gas transfer velocity parameterization, compared to a gridded distribution based on observations [Key *et al.*, 2004]. For MITgcm, modeled distributions derived using both full transport fields and regional pulse functions are shown; we used the latter to model bomb radiocarbon uptake. We used MOM for reconstructing preindustrial sea-surface $\Delta^{14}\text{C}$ and $\delta^{13}\text{C}$. The modeled distributions are summed only over the grid cells for which the gridded distribution is available, largely excluding, for example, the Arctic Ocean.

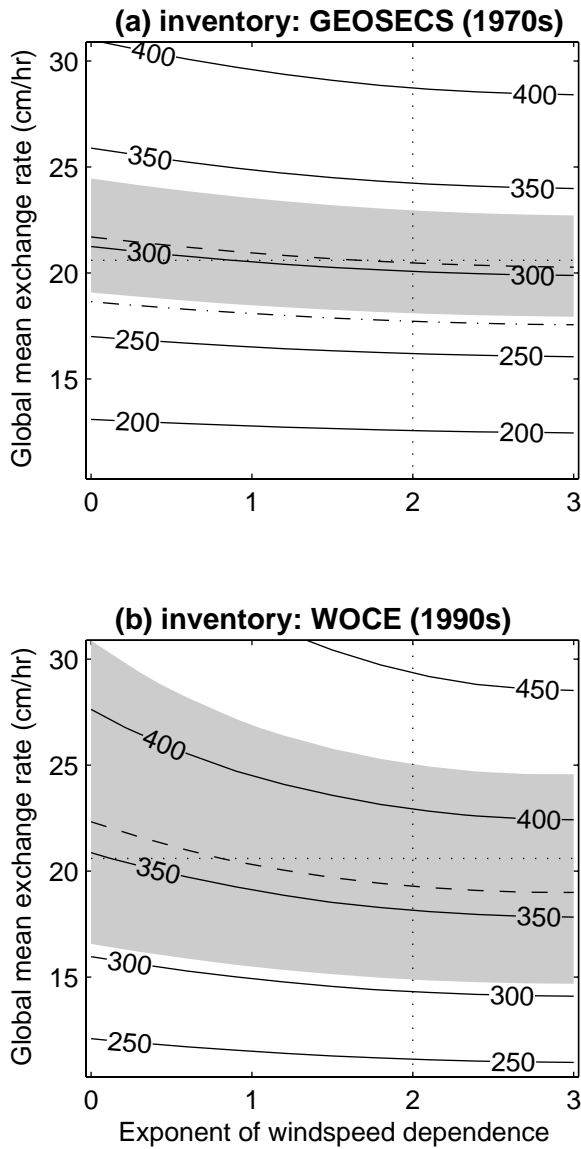


Figure 5. Our model-predicted total ocean bomb radiocarbon amount, in 10^{26} atoms, at the middle of the (a) GEOSECS and (b) WOCE measurement programs (1975.0 and 1994.5, respectively), when the model is run with air-sea gas exchange following Equation 4 with different values of the windspeed dependence exponent n and the global mean rate \bar{k} . Corresponding observation-based amounts from *Broecker et al.* [1995] ($305 \pm 30 \times 10^{26}$ atoms; dashed line and shading in (a)), *Peacock* [2004] ($270 \pm 25 \times 10^{26}$ atoms; dot-dashed line in (a)), and *Key et al.* [2004] ($364 \pm 55 \times 10^{26}$ atoms; dashed line and shading in (b)) are also shown. The dotted lines show the values for these parameters used in OCMIP [*Wanninkhof*, 1992].

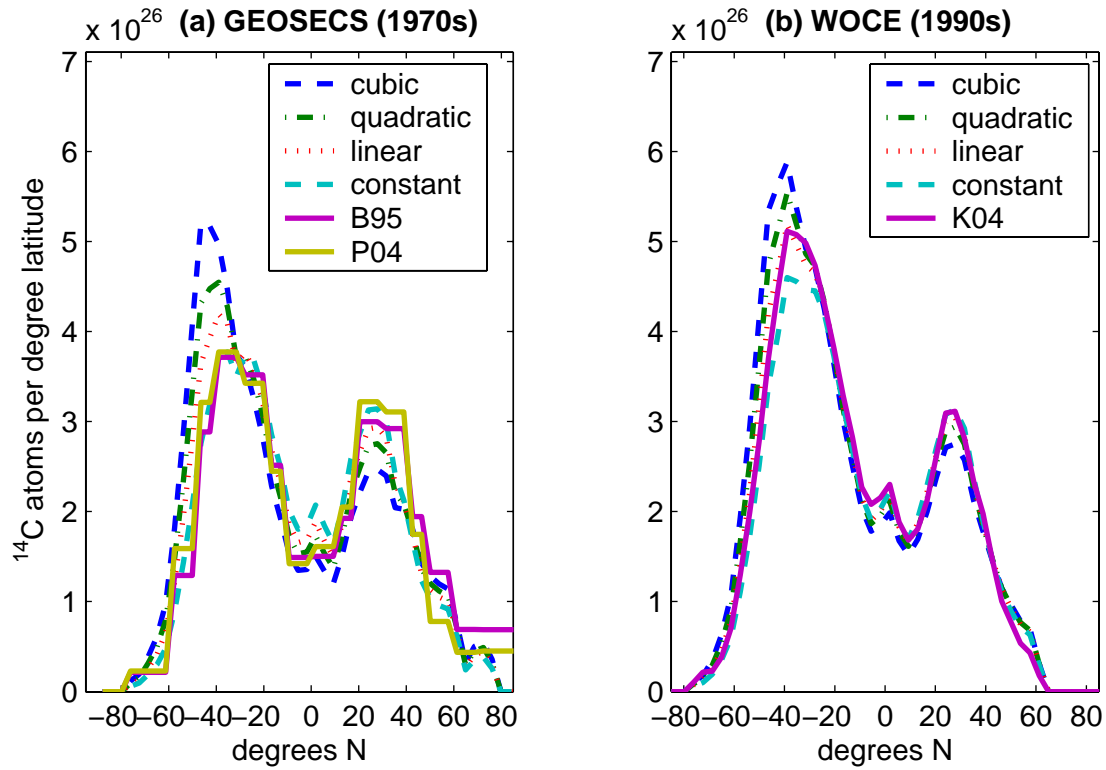


Figure 6. Modeled latitudinal distribution of bomb carbon-14 in the ocean, for a global mean gas transfer velocity \bar{k} of 20.6 cm / hour and a dependence on windspeed ranging from cubic to none ($n=3, 2, 1$ or 0). A lower dependence on windspeed leads to relatively less uptake at the midlatitudes and more near the equator. In panel a, the 1975.0 modeled distribution is compared with extrapolations from GEOSECS observations in 10° bands by *Broecker et al.* [1995] and by *Peacock* [2004] (mean of her CFC- and anthropogenic CO_2 -based extrapolation approaches). In panel b, the 1994.5 modeled distribution is compared to the GLODAP gridded distribution based on WOCE observations [*Key et al.*, 2004]; the modeled distribution is summed only over the grid cells for which the gridded distribution is available, excluding, for example, the Arctic Ocean.

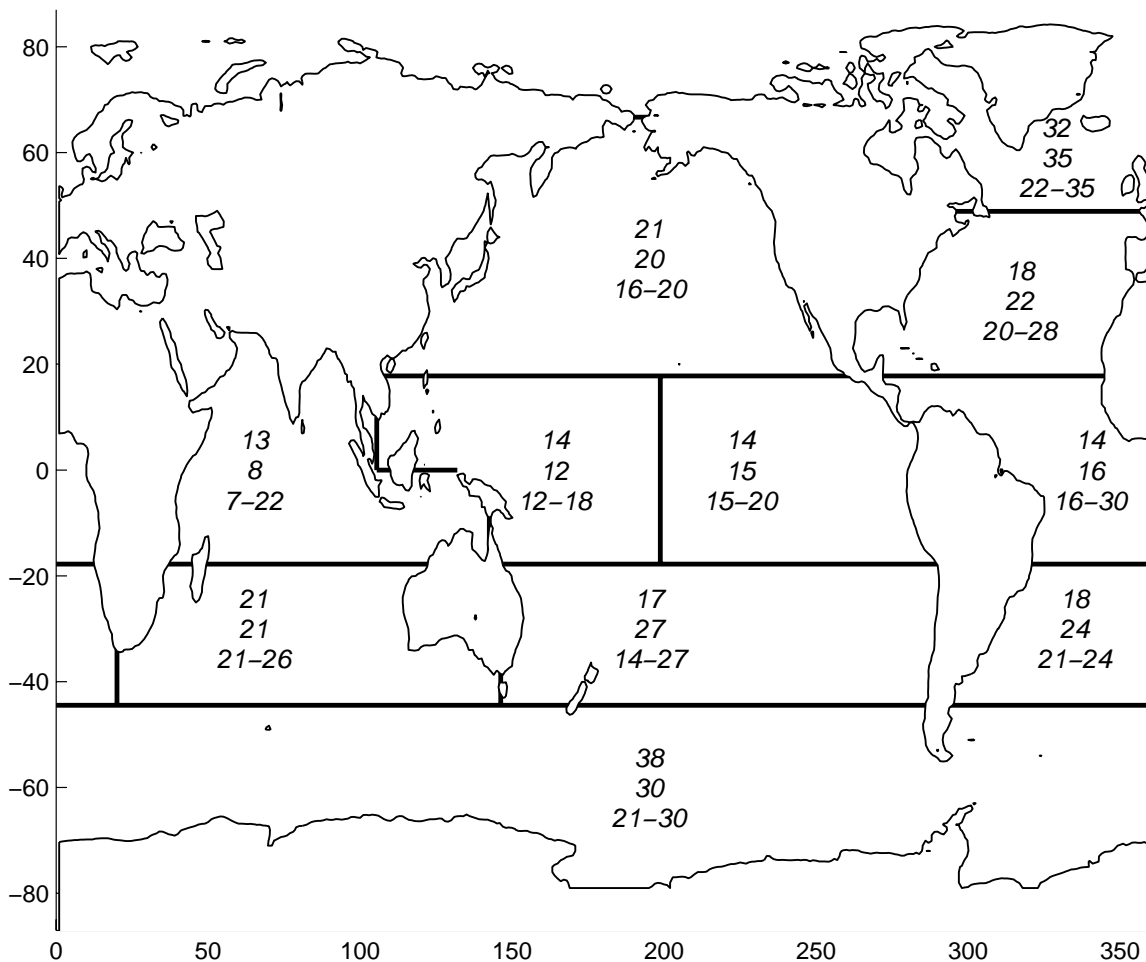


Figure 7. Mean air-sea gas transfer velocities over 11 regions (cm / hour), derived using the quadratic relationship with windspeed of *Wanninkhof* [1992; *Dutay et al.*, 2002] (top row in each region) and estimated by optimizing the fit to 1970s ocean bomb radiocarbon observations where potential alkalinity is used to determine the bomb component (second row); the third row gives a range of optimized fits obtained from variant optimizations that featured fitting integrated vertical profile amounts instead of individual measurements and/or using silicate instead of potential alkalinity or silicate measurements to help determine the bomb component. This range gives a better idea of the actual uncertainty in our results than the uncertainty obtained by assuming error in the measurements to be uncorrelated, which is around 1 cm / hour for each region.

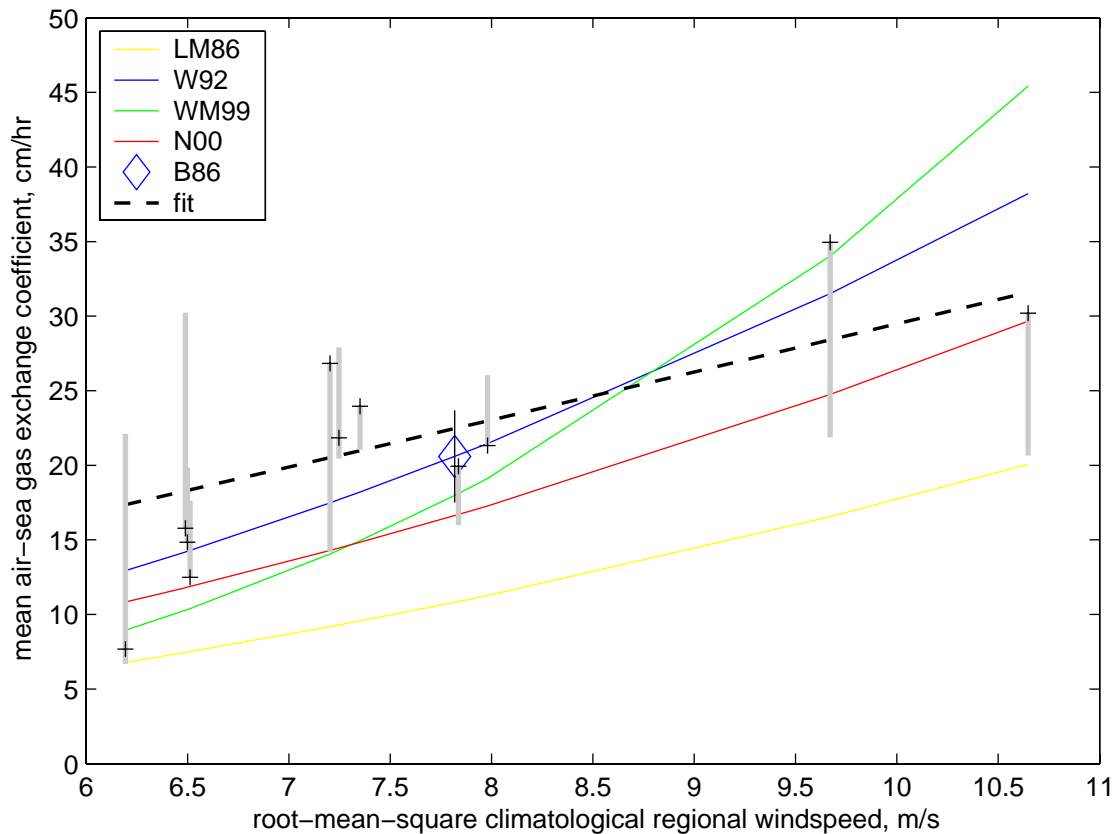


Figure 8. Regional air-sea gas transfer velocity estimated from optimizing the fit to ocean bomb carbon-14 measurements plotted against regional root mean square windspeed (crosses, with gray bars indicating the range from different optimization cases, which is taken to be the 1 standard deviation uncertainty range). Selected published formulations of air-sea gas exchange as a function of windspeed are shown for comparison: the piecewise linear relationship from *Liss and Merlivat* [1986] (here approximated as quadratic, following *Wanninkhof* [1992]); the quadratic relationship of *Wanninkhof* [1992]; the cubic relationship of *Wanninkhof and McGillis* [1999]; and the polynomial (quadratic and linear terms) relationship of *Nightingale et al.* [2000]. To graph these formulations, we calculated first and third moments of the windspeed distribution from the mean square (second moment) climatology assuming that windspeeds in each region followed a Rayleigh distribution. The diamond and error bar show, at the global root-mean-square windspeed, the global gas transfer velocity estimated from ocean radiocarbon evidence by *Broecker et al.* [1986]. The best-fit power law relationship to the regional windspeed is also drawn (dashed curve): it has an exponent of 1.11 ± 0.37 and a global mean of 20.6 ± 0.6 cm / hour.

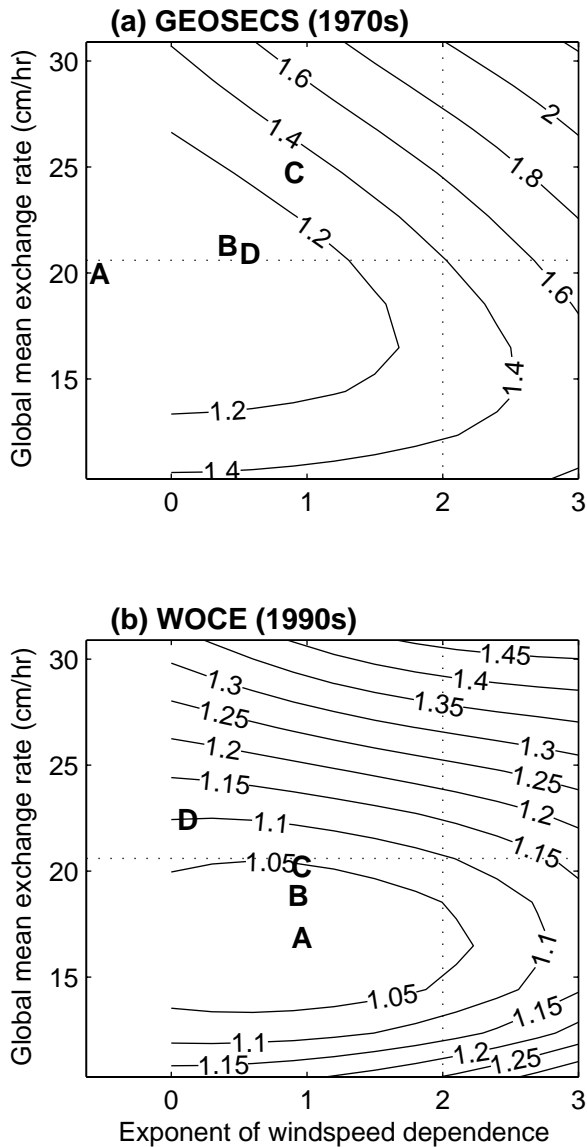


Figure 9. Minimizing the misfit of predicted vs. observed gas exchange as a function of the air-sea gas transfer velocity windspeed dependence exponent n and the global mean rate \bar{k} . (a) Misfit with GEOSECS (1970s) bomb radiocarbon observations; (b) misfit with WOCE (mostly 1990s) observations. The letters show the minimum-misfit point for different considered. The cases are: fit against individual measurements using either potential alkalinity (A) or silica (B) to estimate the background $\Delta^{14}\text{C}$; or fit against column amount computed from measured vertical profiles, again using potential alkalinity (C) or silica (D). The contour lines show the misfit function values, relative to their minima, for the case marked A. The dotted lines show the *Wanninkhof* [1992] values for the global mean gas transfer velocity and for the windspeed dependence exponent.

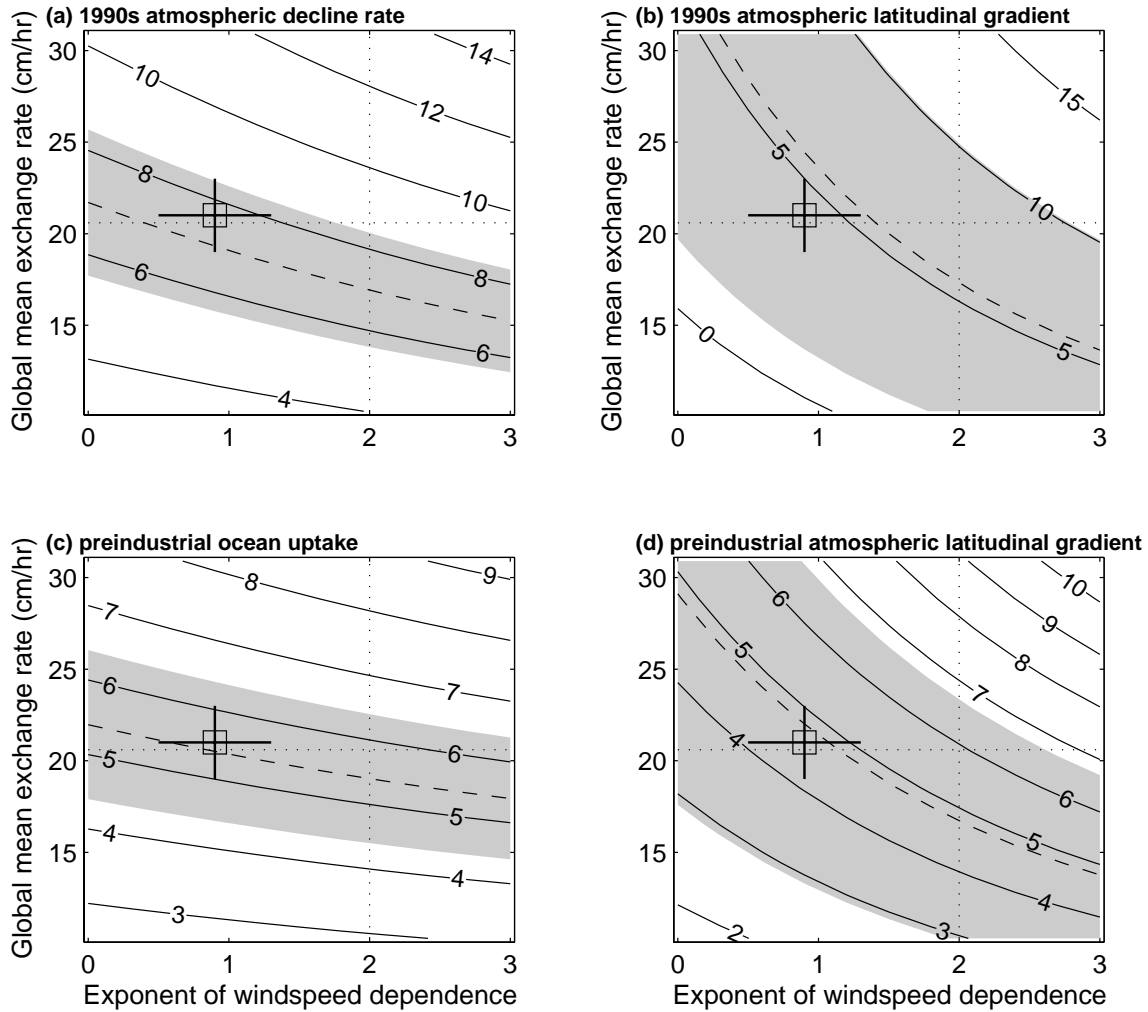


Figure 10. Effect of the air-sea gas exchange parameterization on predicted total ocean ^{14}C uptake and on latitudinal gradients in atmospheric $\Delta^{14}\text{C}$. The dotted lines show the *Wanninkhof* [1992] values for the global mean gas transfer velocity and for the windspeed dependence exponent. The square and error bars mark the parameter values that we found to best fit ocean bomb radiocarbon measurements. The dashed lines show the approximate uptake or latitudinal gradients inferred from observations, and the shading shows the 1 standard deviation uncertainty range both by measurement error and by error in other components of the measured-modeled comparison, such as atmospheric transport. (a) Decline rate (in $\text{‰} / \text{year}$) of atmospheric $\Delta^{14}\text{C}$ around 1994, based on sea-surface $\Delta^{14}\text{C}$ interpolated from WOCE observations, atmospheric $\Delta^{14}\text{C}$ from atmospheric observations, and estimates of isotope fluxes due to biosphere exchange, cosmogenic ^{14}C production and fossil carbon emissions. Observations yield a decline rate of $7.0 \pm 1.4 \text{‰} / \text{year}$. (b) Latitudinal gradient in mean-annual atmospheric $\Delta^{14}\text{C}$ (Llano de Hato, Venezuela [8°N] – Macquarie Island [54°S]) around 1994, based on sea-surface $\Delta^{14}\text{C}$ interpolated from WOCE observations, atmospheric $\Delta^{14}\text{C}$ from atmospheric observations, and estimates of isotope fluxes due to biosphere exchange, cosmogenic ^{14}C production, and fossil carbon emissions, calculated with the atmospheric transport model MATCH. Observations reported by *Levin and Hesshaimer* [2000] yield a difference of $5.6 \pm 4.5 \text{‰}$.

(c) Steady-state ocean ^{14}C uptake (in kg / year) assuming an estimated preindustrial sea-surface $\Delta^{14}\text{C}$ distribution and mean atmospheric $\Delta^{14}\text{C}$ at 0‰. For comparison, 5.4 ± 1 kg / year would be needed to replace the decay of ^{14}C in the ocean DIC pool. (d) Steady-state latitudinal atmospheric $\Delta^{14}\text{C}$ gradient (Britain – New Zealand, in each hemisphere's summer; in permil) calculated with the atmospheric transport model MATCH, assuming an estimated preindustrial sea-surface $\Delta^{14}\text{C}$ distribution and mean atmospheric $\Delta^{14}\text{C}$ at 0‰. For comparison, preindustrial tree-ring measurements reported by *Hogg et al.* [2002] yield a difference of 4.8 ± 1.6 ‰.

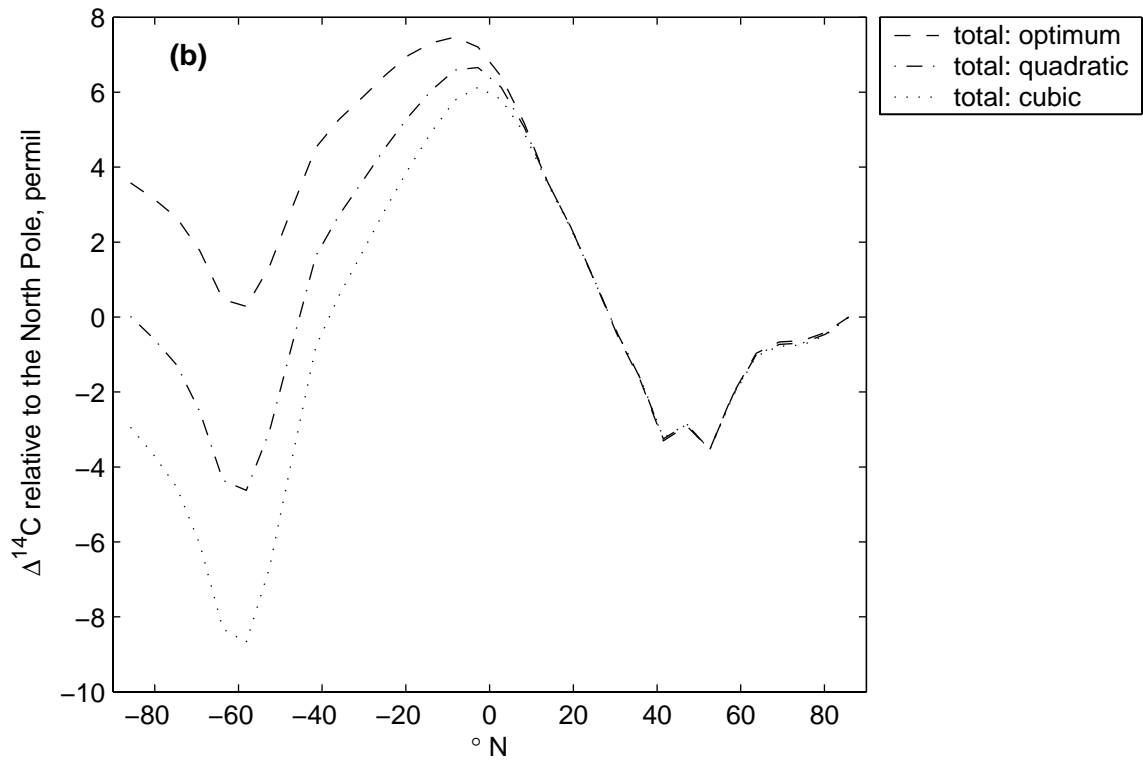
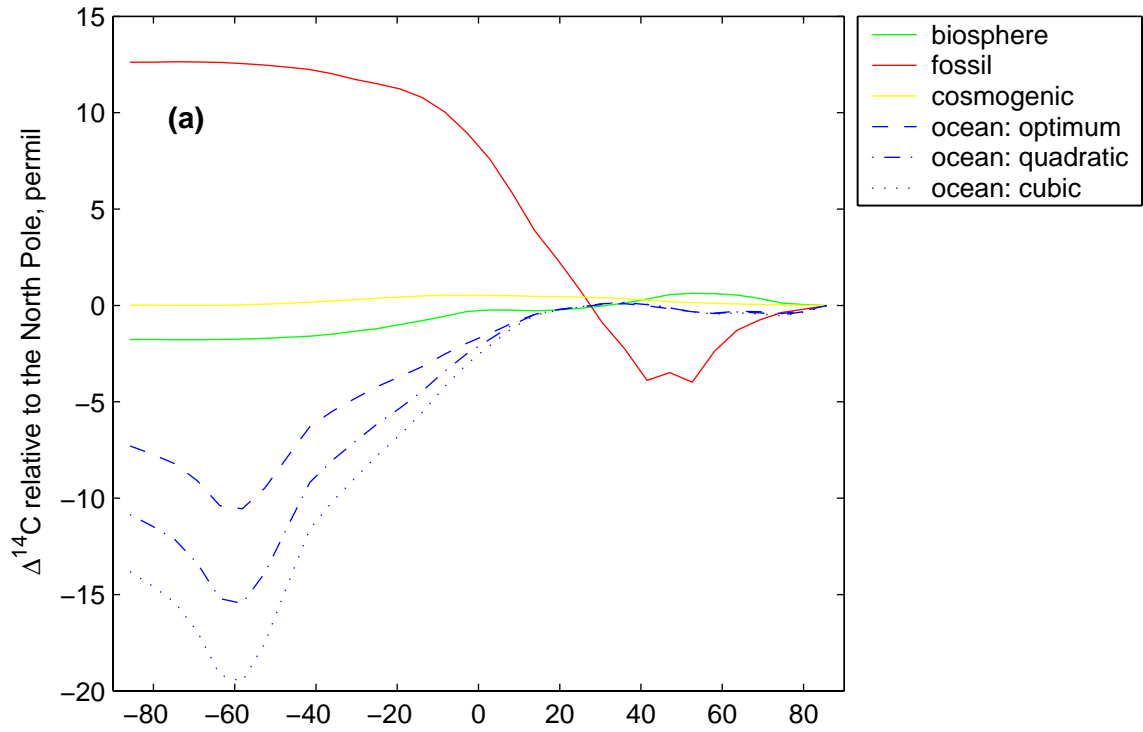


Figure 11. Predicted mean latitudinal gradient in $\Delta^{14}\text{C}$ of atmospheric CO_2 around 1994, taking into account the primary processes likely to cause spatial heterogeneities. We show the effect of modeled ocean uptake using measured sea-surface $\Delta^{14}\text{C}$ [Key *et al.*, 2004] and either our optimized parameterization of the increase of the gas transfer velocity with windspeed (close to linear, with an exponent $n = 0.9$) or quadratic or cubic parameterizations ($n = 2$ or 3). (a) Modeled contribution by process. Fossil fuel emissions, concentrated in the northern midlatitudes, dilute atmospheric ^{14}C , while respired CO_2 from the land biosphere contains high levels of bomb radiocarbon and leads to a smaller enhancement in $\Delta^{14}\text{C}$ over tropical forests and the northern midlatitudes. Exchange with ^{14}C -depleted carbon in the Southern Ocean reduces atmospheric $\Delta^{14}\text{C}$ in the southern midlatitudes, with the modeled magnitude of the depletion depending on the assumed dependence of the air-sea gas transfer velocity on windspeed. (b) Resultant modeled gradient. While the $\Delta^{14}\text{C}$ distribution in the northern hemisphere is unaffected by the assumed form of the air-sea gas transfer velocity, this form has a major influence on the $\Delta^{14}\text{C}$ distribution in the southern hemisphere.

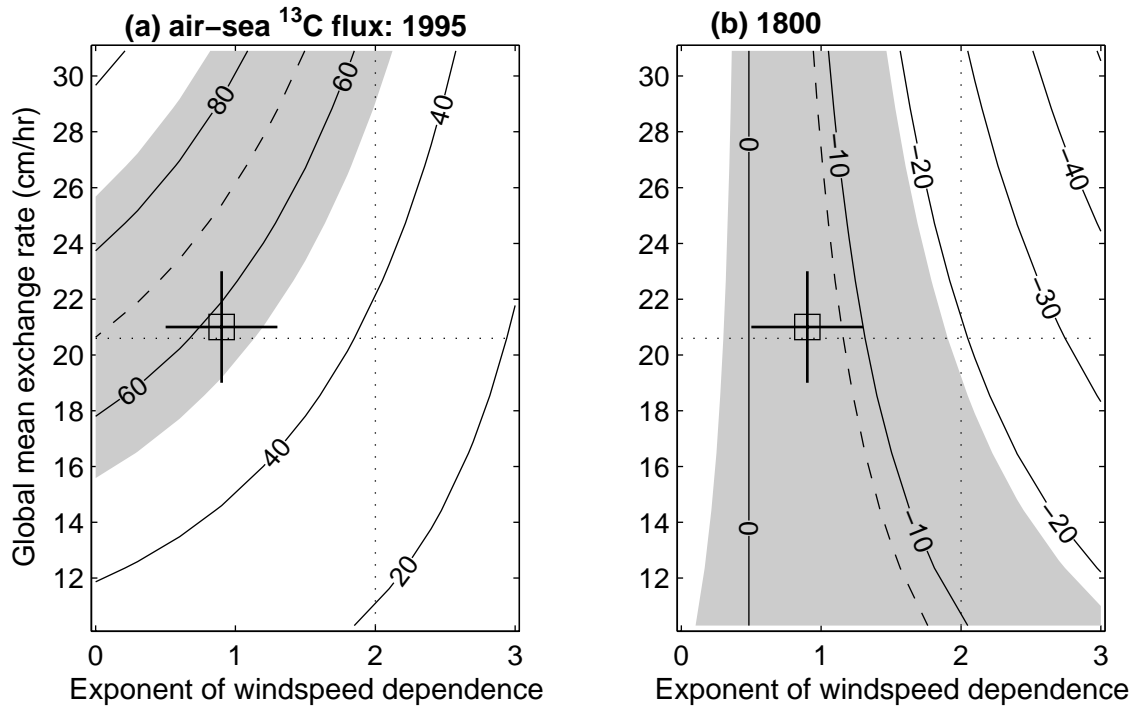


Figure 12. Effect of the air-sea gas exchange parameterization on the ^{13}C isotope flux into the ocean, in Pg C $\%$ / year, derived from observations of sea-surface and atmosphere $\delta^{13}\text{C}$, (a) for the mid-1990s and (b) preindustrially. The dashed line and shading in (a) shows the observation-based estimate (± 1 standard deviation) of 70 ± 17 Pg C $\%$ / year; the corresponding constraint for (b) is -8 ± 10 Pg C $\%$ / year. The dotted lines show the Wanninkhof [1992] values for the global mean gas transfer velocity and for the windspeed dependence exponent. The square and error bars mark the parameter values that we found to best fit ocean bomb radiocarbon measurements.

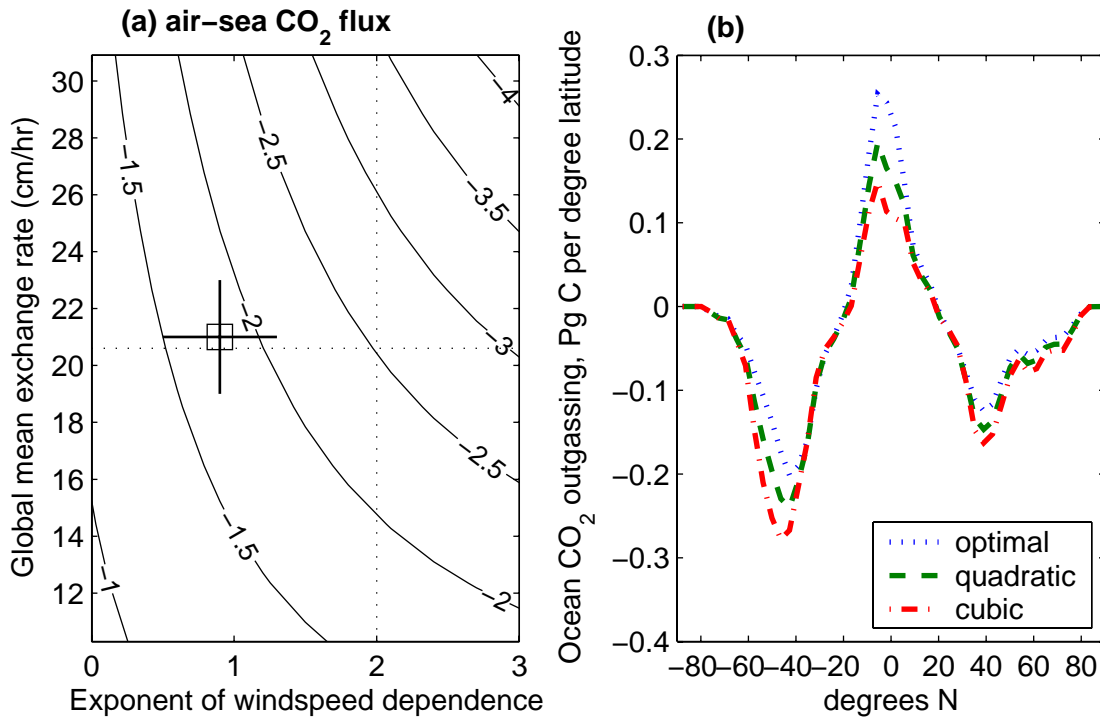


Figure 13. Effect of the air-sea gas transfer velocity parameterization on predicted air-sea flux of CO₂, based on the air-sea $p\text{CO}_2$ climatology prepared by *Takahashi et al.* [2002] for 1995. (a) Predicted global ocean uptake of anthropogenic CO₂ (in Pg C / year) as a function of the air-sea gas exchange parameterization. To obtain the anthropogenic CO₂ flux, we corrected the total flux by 0.7 Pg C / year for the assumed steady-state ocean outgassing that balances an inflow of continental carbon [*Aumont et al.*, 2001]. The dashed lines show the *Wanninkhof* [1992] values for the global mean gas transfer velocity and for the windspeed dependence exponent. The square and error bars mark the parameter values that we found to best fit ocean bomb radiocarbon measurements. Observational estimates of this uptake have been around 2.0-2.4 Pg C / year. (b) Latitudinal distribution of the air-sea flux for our optimized parameter values and for parameterizations of air-sea gas exchange with quadratic or cubic dependences on windspeed.

Table 1. Rate of decline of atmospheric $\Delta^{14}\text{C}$ around 1994

Station	Latitude	$\Delta^{14}\text{C}$ of atmospheric CO_2 (‰)		rate of decline (‰ / year)
		1992.0 ^d	1997.0 ^d	
Schauinsland ^a	48°N	138	102	7.2
Jungfrauoch ^a	47°N	139	105	6.8
Pretoria ^b	26°S	148	117	6.3
Wellington ^c	41°S	153	114	7.7
Mean \pm SD				7.0\pm0.6

a. *Levin and Kromer* [2004].

b. S. Woodbourne, personal communication, updating *Manning et al.* [1990].

c. G. Brailsford, personal communication, updating *Vogel* [1971].

d. For the northern hemisphere stations, calculated as the average of the preceding and subsequent summer (since atmospheric $\Delta^{14}\text{C}$ near the surface is more variable in winter than in summer).

Table 2. Modeled contributions of carbon fluxes to the rate of decline and latitudinal gradient in atmospheric $\Delta^{14}\text{C}$ around 1994

	Growth rate (‰ / year)	Latitudinal gradient^a (‰)
Biosphere ^b	3.7±0.7	2.7±1.2
Fossil fuels ^b	-9.3±0.5	-7.8±1.6
Cosmogenic production ^b	6.2±0.6	0.5±0.6
Ocean		
Linear ^c	-8.2±0.6	8.9±2.6
Quadratic ^c	-9.3±0.7	12.2±3.4
Cubic ^c	-10.3±0.7	15.4±4.3
Model uncertainty^d	±1.3	±3.5
Measured value	-7.0±0.6 ^e	5.6±2.8 ^f
Total uncertainty^g	±1.4	±4.5

a. Annual-mean $\Delta^{14}\text{C}$ at Llano de Hato, Venezuela (9°N), subtracted from that at Macquarie Island (54°S).

b. Modeled effects (see Methods section); 1-SD uncertainties reflect approximate confidence in flux size, plus error in the atmospheric transport model (estimated from the spread in standardized regional pulse functions of models participating in the TransCom 3 intercomparison [Gurney *et al.*, 2003]) in the case of the latitudinal gradient.

c. For air-sea gas transfer velocity formulations with the global mean rate the same as in the OCMIP formulation ($\bar{k} = 20.6$ cm / hour in Equation 3) and a linear, quadratic, or cubic dependence on windspeed ($n = 1, 2$ or 3). The given uncertainties reflect confidence in the air-sea $\Delta^{14}\text{C}$ disequilibrium and in the transport model, assuming that the given formulation of gas exchange is correct.

d. Overall uncertainty in the model prediction: sum of the uncertainties from the different components, assuming the quadratic dependence of air-sea gas exchange on windspeed for the ocean contribution.

e. See Table 1.

f. Levin and Hesshaimer [2000].

g. Model plus measurement uncertainty contributions.

Table 3. Deriving the ^{13}C isotope flux out of the ocean around 1995 from the atmospheric ^{13}C budget

Observed or estimated quantities

Atmospheric CO_2	763.8 ^a ±3.2	Pg C
Fossil CO_2 emissions	6.4 ^b ±0.3	Pg C / year
Ocean anthropogenic CO_2 uptake	2.2 ^c ±0.3	Pg C / year
Atmospheric CO_2 rate of increase	3.2 ^d ±0.3	Pg C / year
Mean $\delta^{13}\text{C}$ of fossil emissions	-28.1±1	‰
Mean $\delta^{13}\text{C}$ of atmospheric CO_2	-7.91 ^e ±0.03	‰
Disequilibrium of terrestrial respiration	0.35 ^f ±0.1	‰
Terrestrial net primary productivity	55.4 ^f ±15	Pg C / year
Terrestrial photosynthesis ^{13}C discrimination	-19±1.5	‰
Rate of change in $\delta^{13}\text{C}$ of atmospheric CO_2	-0.018 ^e ±0.005	‰
River flow of terrestrial organic matter into ocean	0.4 ^g ±0.2	Pg C / year
Derived quantities		
Land biosphere CO_2 uptake	1.0±0.5	Pg C / year
Atmospheric ^{13}C budget: isotope fluxes		
Fossil fuels	-128±9	Pg C ‰ / year
Land biosphere, from isotopic disequilibrium	19±8	Pg C ‰ / year
Land biosphere, from fractionation in net CO_2 uptake	18±10	Pg C ‰ / year
Storage in atmosphere (change in $\delta^{13}\text{C}$)	-14±4	Pg C ‰ / year
Inferred disequilibrium isotope flux from ocean	77±16	Pg C ‰ / year
Sea-air isotope flux to balance river flow at steady state	-8±4	Pg C ‰ / year
Inferred total air-sea isotope flux	70±17	Pg C ‰ / year

Adopted values and 1-SD uncertainties were mostly based on those used in the similar calculations by *Heimann and Maier-Reimer* [1996] and *Gruber and Keeling* [2001], except as specified below.

a. From 1995 means of NOAA-CMDL flask measurements [*Conway et al.*, 1994] for remote stations, binned by latitude and averaged.

b. *Marland et al.* [2005]

c. *Mikaloff Fletcher et al* [in press]

d. Change over the 1990s in NOAA-CMDL flask measurements [*Conway et al.*, 1994] for remote stations, binned by latitude and averaged.

e. 1995 means and change over the 1990s in measurements from the CSIRO [*Francey et al.*, 2001] and Scripps [*Keeling et al.*, 1995] station networks, binned by latitude and averaged

f. CASA [*Potter et al.*, 1993] plant and soil carbon model; the disequilibrium was derived by weighting respiration pulse functions from CASA [*Thompson and Randerson*, 1999] with a time series of change in atmospheric $\delta^{13}\text{C}$ [*Francey et al.*, 1999].

g. *Aumont et al.* [2001]; we assumed this flux to have the same $\delta^{13}\text{C}$ as mean terrestrial photosynthesis

Table 4. Summary of ^{14}C and ^{13}C constraints on the global mean air-sea gas transfer velocity \bar{k} and its windspeed dependence exponent n

Constraint	Implied \bar{k} (cm / hour)	Implied n
Ocean bomb ^{14}C measurements		
Ocean total amount (WOCE)	15-31	
Fit of regional gas transfer velocities	20.6±0.6	1.11±0.37
Fit of \bar{k} , n directly	20.7±2.4	0.61±0.40
Overall	21±2	0.9±0.4
Other ^{14}C and ^{13}C measurements *		
Atmospheric $\Delta^{14}\text{C}$: 1990s decline rate	19±4	0.3 (0-1.6)
Atmospheric $\Delta^{14}\text{C}$: 1990s latitudinal gradient	24±11	1.3 (0-2.7)
Preindustrial ocean ^{14}C uptake	21±4	
Preindustrial atmospheric $\Delta^{14}\text{C}$ latitudinal gradient	22±9	1.1 (0-2.5)
Air-sea ^{13}C isotope flux, 1990s	25±6	0.1 (0-1.2)
Air-sea ^{13}C isotope flux, preindustrial		1.1 (0.3-1.9)

The ranges or 1- σ uncertainties given for the implied values of \bar{k} and n are based on our estimates of measurement and model uncertainties, and/or on the spread between fits using different assumptions; see text for details.

* These measurements typically imply a range of compatible (\bar{k} , n) pairs (shown as the area shaded gray in Figure 10 and 12). The implied values given here are the compatible values of \bar{k} or n if the other parameter is set to the best-fit value determined from the ocean bomb radiocarbon distribution (i.e. $n = 0.9$ or $\bar{k} = 21$ cm / hour), which independently constrains both parameters. We left cells blank if the measurement does not meaningfully constrain \bar{k} or n within the range of $\bar{k} = 10-31$ cm / hour and $n = 0-3$.

References

- Andres, R. J., G. Marland, I. Fung, et al. (1996), A $1^{\circ} \times 1^{\circ}$ distribution of carbon dioxide emissions from fossil fuel consumption and cement manufacture, 1950-1990, *Global Biogeochem. Cycles*, 10(3), 419-429.
- Asher, W., Q. Wang, E. C. Monahan, et al. (1998), Estimation of air-sea gas transfer velocities from apparent microwave brightness temperature, *Marine Tech. Soc. J.*, 32(2), 32-40.
- Aster, R. C., B. Borchers and C. H. Thurber (2005), *Parameter Estimation and Inverse Problems*, 301 pp., Elsevier Academic Press.
- Aumont, O., J. C. Orr, P. Monfray, et al. (2001), Riverine-driven interhemispheric transport of carbon, *Global Biogeochem. Cycles*, 15(2), 393-405.
- Bacastow, R. B., C. D. Keeling, T. J. Lueker, et al. (1996), The C-13 Suess effect in the world surface oceans and its implications for oceanic uptake of CO₂: Analysis of observations at Bermuda, *Global Biogeochem. Cycles*, 10(2), 335-346.
- Bates, N. R. (2002), Interannual variability in the global uptake of CO₂, *Geophys. Res. Lett.*, 29(5).
- Bousquet, P., P. Peylin, P. Ciais, et al. (2000), Regional changes in carbon dioxide fluxes of land and oceans since 1980, *Science*, 290(5495), 1342-1346.
- Boutin, J. and J. Etcheto (1996), Consistency of Geosat, SSM/I, and ERS-1 global surface wind speeds - Comparison with in situ data, *Journal of Atmospheric and Oceanic Technology*, 13(1), 183-197.
- Boutin, J. and J. Etcheto (1997), Long-term variability of the air-sea CO₂ exchange coefficient: Consequences for the CO₂ fluxes in the equatorial Pacific ocean, *Global Biogeochem. Cycles*, 11(3), 453-470.
- Boyer, T. P., C. Stephens, J. I. Antonov, et al. (2002), *World Ocean Atlas 2001, Volume 2: Salinity*, 165 pp., US Government Printing Office, Washington.
- Braziunas, T. F., I. Y. Fung and M. Stuiver (1995), The preindustrial atmospheric ¹⁴CO₂ latitudinal gradient as related to exchanges among atmospheric, oceanic, and terrestrial reservoirs, *Global Biogeochem. Cycles*, 9(4), 565-584.
- Broecker, W., R. Gerard, M. Ewing, et al. (1960), Natural Radiocarbon in the Atlantic Ocean, *J. Geophys. Res.*, 65(9), 2903-2931.
- Broecker, W. S., J. R. Ledwell, T. Takahashi, et al. (1986), Isotopic versus micrometeorological ocean CO₂ fluxes - a serious conflict, *J. Geophys. Res.*, 91(C9), 517-527.
- Broecker, W. S. and T.-H. Peng (1982), *Tracers in the sea*, 690 pp., Lamont-Doherty Geological Observatory, Palisades, NY.
- Broecker, W. S., T. H. Peng, G. Ostlund, et al. (1985), The distribution of bomb radiocarbon in the ocean, *J. Geophys. Res.*, 90(C4), 6953-6970.
- Broecker, W. S., S. Sutherland, W. Smethie, et al. (1995), Oceanic radiocarbon - Separation of the natural and bomb components, *Global Biogeochem. Cycles*, 9(2), 263-288.
- Caldeira, K., G. H. Rau and P. B. Duffy (1998), Predicted net efflux of radiocarbon from the ocean and increase in atmospheric radiocarbon content, *Geophys. Res. Lett.*, 25(20), 3811-3814.

- Caldeira, K. and M. E. Wickett (2003), Anthropogenic carbon and ocean pH, *Nature*, 425(6956), 365-365.
- Conway, T. J., P. P. Tans, L. S. Waterman, et al. (1994), Evidence for interannual variability of the carbon cycle from National Oceanic and Atmospheric Administration/Climate Monitoring and Diagnostics Laboratory Global Air Sampling Network, *J. Geophys. Res.*, 99(D11), 23831-23855.
- Craig, H. (1957), The natural distribution of radiocarbon and the exchange time of carbon dioxide between the atmosphere and the sea, *Tellus*, 9, 1-17.
- Damon, P. E. and R. E. Sternberg (1989), Global production and decay of radiocarbon, *Radiocarbon*, 31(3), 697-703.
- Donelan, M. A., B. K. Haus, N. Reul, et al. (2004), On the limiting aerodynamic roughness of the ocean in very strong winds, *Geophys. Res. Lett.*, 31(18).
- Druffel, E. M. and H. E. Suess (1983), On the radiocarbon record in banded corals: Exchange parameters and net transport of $^{14}\text{CO}_2$ between atmosphere and surface ocean, *Journal of Geophysical Research-Oceans and Atmospheres*, 88(NC2), 1271-1280.
- Druffel, E. R. M. (1987), Bomb radiocarbon in the Pacific: Annual and seasonal timescale variations, *J. Mar. Res.*, 45, 667-698.
- Druffel, E. R. M. (1989), Decade time scale variability of ventilation in the North Atlantic: High-precision measurements of bomb radiocarbon in banded corals, *J. Geophys. Res.*, 94(C3), 3271-3285.
- Druffel, E. R. M. and S. Griffin (1995), Regional variability of surface ocean radiocarbon from southern great barrier reef corals, *Radiocarbon*, 37(2), 517-524.
- Dutay, J. C., J. L. Bullister, S. C. Doney, et al. (2002), Evaluation of ocean model ventilation with CFC-11: comparison of 13 global ocean models, *Ocean Modelling*, 4(2), 89-120.
- England, M. H., V. Garçon and J. F. Minster (1994), Chlorofluorocarbon uptake in a world ocean model 1. Sensitivity to the surface gas forcing, *J. Geophys. Res.*, 99(C12), 25215-25233.
- Esbensen, S. K. and Y. Kushnir (1981), *The Heat Budget of the Global Ocean: An Atlas Based on Estimates from Marine Surface Observations*, Oregon State University, Corvallis.
- Fairall, C. W., J. E. Hare, J. B. Edson, et al. (2000), Parameterization and micrometeorological measurement of air-sea gas transfer, *Boundary-Layer Meteorology*, 96(1-2), 63-105.
- Fasham, M. J. R. (2003), *Ocean biogeochemistry : the role of the ocean carbon cycle in global change*, 297 pp., Springer, Berlin; New York.
- Feely, R. A., C. L. Sabine, K. Lee, et al. (2004a), Impact of anthropogenic CO_2 on the CaCO_3 system in the oceans, *Science*, 305(5682), 362-366.
- Feely, R. A., R. Wanninkhof, W. McGillis, et al. (2004b), Effects of wind speed and gas exchange parameterizations on the air-sea CO_2 fluxes in the equatorial Pacific Ocean, *J. Geophys. Res.*, 109(C8).
- Feely, R. A., R. Wanninkhof, T. Takahashi, et al. (1999), Influence of El Niño on the equatorial Pacific contribution to atmospheric CO_2 accumulation, *Nature*, 398(6728), 597-601.

- Francey, R. J., C. E. Allison, D. M. Etheridge, et al. (1999), A 1000-year high precision record of $\delta^{13}\text{C}$ in atmospheric CO_2 , *Tellus*, 51(2), 170-193.
- Francey, R. J., C. E. Allison, C. M. Trudinger, et al. (2001), The interannual variation in global atmospheric $\delta^{13}\text{C}$ and its link to net terrestrial exchange, in *Sixth International Carbon Dioxide Conference, Extended Abstracts*, pp. 43-46, Organizing Committee of Sixth International Carbon Dioxide Conference, Sendai, Japan.
- Frank, N., M. Paterne, L. Ayliffe, et al. (2004), Eastern North Atlantic deep-sea corals: tracing upper intermediate water $\Delta\text{C-14}$ during the Holocene, *Earth Planet. Sci. Lett.*, 219(3-4), 297-309.
- Frew, N. M., E. J. Bock, U. Schimpf, et al. (2004), Air-sea gas transfer: Its dependence on wind stress, small-scale roughness, and surface films, *J. Geophys. Res.*, 109(C8).
- Frost, T. and R. C. Upstill-Goddard (1999), Air-sea gas exchange into the millennium: Progress and uncertainties, in *Oceanography and Marine Biology, Vol 37*, pp. 1-45.
- Garabetian, F. (1991), ^{14}C -glucose uptake and ^{14}C - CO_2 production in surface microlayer and surface-water samples: influence of UV and visible radiation, *Marine Ecology-Progress Series*, 77(1), 21-26.
- Gloor, M., N. Gruber, T. M. C. Hughes, et al. (2001), Estimating net air-sea fluxes from ocean bulk data: Methodology and application to the heat cycle, *Global Biogeochem. Cycles*, 15(4), 767-782.
- Gloor, M., N. Gruber, J. Sarmiento, et al. (2003), A first estimate of present and preindustrial air-sea CO_2 flux patterns based on ocean interior carbon measurements and models, *Geophys. Res. Lett.*, 30(1), art. no.-1010.
- Goldstein, S. J., D. W. Lea, S. Chakraborty, et al. (2001), Uranium-series and radiocarbon geochronology of deep-sea corals: implications for Southern Ocean ventilation rates and the oceanic carbon cycle, *Earth Planet. Sci. Lett.*, 193(1-2), 167-182.
- Goslar, T. (2001), Absolute production of radiocarbon and the long-term trend of atmospheric radiocarbon, *Radiocarbon*, 43(2B), 743-749.
- Gruber, N., M. Gloor, S. M. Fan, et al. (2001), Air-sea flux of oxygen estimated from bulk data: Implications for the marine and atmospheric oxygen cycles, *Global Biogeochem. Cycles*, 15(4), 783-803.
- Gruber, N. and C. D. Keeling (2001), An improved estimate of the isotopic air-sea disequilibrium of CO_2 : Implications for the oceanic uptake of anthropogenic CO_2 , *Geophys. Res. Lett.*, 28(3), 555-558.
- Gruber, N., C. D. Keeling, R. B. Bacastow, et al. (1999), Spatiotemporal patterns of carbon-13 in the global surface oceans and the oceanic Suess effect, *Global Biogeochem. Cycles*, 13(2), 307-335.
- Gruber, N., J. L. Sarmiento and T. F. Stocker (1996), An improved method for detecting anthropogenic CO_2 in the oceans, *Global Biogeochem. Cycles*, 10(4), 809-837.
- Gurney, K. R., R. M. Law, A. S. Denning, et al. (2002), Towards robust regional estimates of CO_2 sources and sinks using atmospheric transport models, *Nature*, 415(6872), 626-630.

- Gurney, K. R., R. M. Law, A. S. Denning, et al. (2003), TransCom 3 CO₂ inversion intercomparison: 1. Annual mean control results and sensitivity to transport and prior flux information, *Tellus*, 55(B2), 555-579.
- Heimann, M. and E. Maier-Reimer (1996), On the relations between the oceanic uptake of CO₂ and its carbon isotopes, *Global Biogeochem. Cycles*, 10(1), 89-110.
- Heimann, M. and P. Monfray (1989), Spatial and Temporal Variation of the Gas Exchange Coefficient for CO₂: 1. Data Analysis and Global Validation, pp. 29, Max-Planck-Institut für Meteorologie, Hamburg.
- Hesshaimer, V., M. Heimann and I. Levin (1994), Radiocarbon evidence for a smaller oceanic carbon-dioxide sink than previously believed, *Nature*, 370(6486), 201-203.
- Hogg, A. G., F. G. McCormac, T. F. G. Higham, et al. (2002), High-precision radiocarbon measurements of contemporaneous tree-ring dated wood from the British Isles and New Zealand: AD 1850-950, *Radiocarbon*, 44(3), 633-640.
- Hua, Q. and M. Barbetti (2004), Review of tropospheric bomb ¹⁴C data for carbon cycle modeling and age calibration purposes, *Radiocarbon*, 46(3), 1273-1298.
- Hua, Q., M. Barbetti, M. Worbes, et al. (1999), Review of radiocarbon data from atmospheric and tree ring samples for the period 1945-1997 AD, *Iawa J.*, 20(3), 261-283.
- Ito, T., J. Marshall and M. Follows (2004), What controls the uptake of transient tracers in the Southern Ocean?, *Global Biogeochem. Cycles*, 18(2).
- Jähne, B. and H. Haussecker (1998), Air-water gas exchange, *Annual Review of Fluid Mechanics*, 30, 443-468.
- Joos, F. (1996), An efficient and accurate representation of complex oceanic and biospheric models of anthropogenic carbon uptake, *Tellus. Series B, Chemical and physical meteorology*, 48(3), 397-417.
- Keeling, C. D., R. B. Bacastow, A. E. Bainbridge, et al. (1976), Atmospheric carbon-dioxide variations at Mauna-Loa Observatory, Hawaii, *Tellus*, 28(6), 538-551.
- Keeling, C. D., T. P. Whorf, M. Wahlen, et al. (1995), Interannual Extremes in the Rate of Rise of Atmospheric Carbon-Dioxide since 1980, *Nature*, 375(6533), 666-670.
- Key, R. M., A. Kozyr, C. L. Sabine, et al. (2004), A global ocean carbon climatology: Results from Global Data Analysis Project (GLODAP), *Global Biogeochemical Cycles*, 18(4), GB4031.
- Key, R. M., P. D. Quay, P. Schlosser, et al. (2002), WOCE radiocarbon IV: Pacific Ocean results; P10, P13N, P14C, P18, P19 & S4P, *Radiocarbon*, 44(1), 239-392.
- Komori, S., R. Nagaosa and Y. Murakami (1993), Turbulence structure and mass-transfer across a sheared air-water interface in wind-driven turbulence, *J. Fluid Mech.*, 249, 161-183.
- Krakauer, N. Y., T. Schneider, J. T. Randerson, et al. (2004), Using generalized cross-validation to select parameters in inversions for regional carbon fluxes, *Geophys. Res. Lett.*, 31(19).
- Levin, I. and V. Hesshaimer (2000), Radiocarbon - A unique tracer of global carbon cycle dynamics, *Radiocarbon*, 42(1), 69-80.
- Levin, I. and B. Kromer (2004), The Tropospheric ¹⁴CO₂ level in Mid-Latitudes of the Northern Hemisphere (1959–2003), *Radiocarbon*, 46(3), 1261-1272.

- Levin, I., B. Kromer, M. Schmidt, et al. (2003), A novel approach for independent budgeting of fossil fuel CO₂ over Europe by ¹⁴CO₂ observations, *Geophys. Res. Lett.*, 30(23), art. no.-2194.
- Levin, I., B. Kromer, D. Wagenbach, et al. (1987), Carbon isotope measurements of atmospheric CO₂ at a coastal station in Antarctica, *Tellus*, 39B(1-2), 89-95.
- Lingenfelter, R. E. (1963), Production of carbon-14 by cosmic-ray neutrons, *Reviews of Geophysics*, 1(1), 35-55.
- Linick, T. W. (1980), Bomb-produced C-14 in the surface-water of the Pacific Ocean, *Radiocarbon*, 22(3), 599-606.
- Liss, P. S., A. L. Chuck, S. M. Turner, et al. (2004), Air-sea gas exchange in Antarctic waters, *Antarctic Sci.*, 16(4), 517-529.
- Liss, P. S. and L. Merlivat (1986), Air-sea gas exchange rates: introduction and synthesis, in *The role of air-sea exchange in geochemical cycling*, edited by P. Buat-Ménard, pp. 113-129, D. Reidel, Dordrecht.
- Mahowald, N. M., P. J. Rasch, B. E. Eaton, et al. (1997), Transport of ²²²radon to the remote troposphere using the Model of Atmospheric Transport and Chemistry and assimilated winds from ECMWF and the National Center for Environmental Prediction/NCAR, *J. Geophys. Res.*, 102(D23), 28139-28151.
- Manning, M. R., D. C. Lowe, W. H. Melhuish, et al. (1990), The use of radiocarbon measurements in atmospheric studies, *Radiocarbon*, 32(1), 37-58.
- Marland, G., T. A. Boden and R. J. Andres (2005), Global, Regional, and National Fossil Fuel CO₂ Emissions, in *Trends: A Compendium of Data on Global Change.*, Carbon Dioxide Information Analysis Center, Oak Ridge National Laboratory, U.S. Department of Energy.
- Marshall, J., A. Adcroft, C. Hill, et al. (1997), A finite-volume, incompressible Navier Stokes model for studies of the ocean on parallel computers, *J. Geophys. Res.*, 102(C3), 5753-5766.
- Masiello, C. A., E. R. M. Druffel and J. E. Bauer (1998), Physical controls on dissolved inorganic radiocarbon variability in the California Current, *Deep-Sea Res.*, 45(4-5), 617-642.
- McGillis, W. R., J. B. Edson, J. E. Hare, et al. (2001), Direct covariance air-sea CO₂ fluxes, *J. Geophys. Res.*, 106(C8), 16729-16745.
- McGillis, W. R., J. B. Edson, C. J. Zappa, et al. (2004), Air-sea CO₂ exchange in the equatorial Pacific, *J. Geophys. Res.*, 109(C8).
- McNeil, B. I., R. J. Matear, R. M. Key, et al. (2003), Anthropogenic CO₂ uptake by the ocean based on the global chlorofluorocarbon data set, *Science*, 299(5604), 235-239.
- Michalak, A. M., L. Bruhwiler and P. P. Tans (2004), A geostatistical approach to surface flux estimation of atmospheric trace gases, *J. Geophys. Res.*, 109(D14).
- Mikaloff Fletcher, S. E., N. Gruber, A. R. Jacobson, et al. (in press), Inverse estimates of anthropogenic CO₂ uptake, transport, and storage by the ocean, *Global Biogeochem. Cycles*, doi: 10.1029/2005GB002530.
- Monahan, E. C. (2002), Oceanic whitecaps: Sea surface features detectable via satellite that are indicators of the magnitude of the air-sea gas transfer coefficient, *Proc. Indian Acad. Sci.-Earth Planet. Sci.*, 111(3), 315-319.

- Murnane, R. J., J. L. Sarmiento and C. Le Quéré (1999), Spatial distribution of air-sea CO₂ fluxes and the interhemispheric transport of carbon by the oceans, *Global Biogeochem. Cycles*, 13(2), 287-305.
- Nightingale, P. D., G. Malin, C. S. Law, et al. (2000), In situ evaluation of air-sea gas exchange parameterizations using novel conservative and volatile tracers, *Global Biogeochem. Cycles*, 14(1), 373-387.
- Nydal, R. (2000), Radiocarbon in the ocean, *Radiocarbon*, 42(1), 81-98.
- Olsen, A., R. Wanninkhof, J. A. Trinanes, et al. (2005), The effect of wind speed products and wind speed-gas exchange relationships on interannual variability of the air-sea CO₂ gas transfer velocity, *Tellus*, 57(2), 95-106.
- Olsen, S. C. and J. T. Randerson (2004), Differences between surface and column atmospheric CO₂ and implications for carbon cycle research, *J. Geophys. Res.*, 109, D02301, doi:10.1029/2003JD003968.
- Orr, J. C., V. J. Fabry, O. Aumont, et al. (2005), Anthropogenic ocean acidification over the twenty-first century and its impact on calcifying organisms, *Nature*, 437(7059), 681-686.
- Orr, J. C., E. Maier-Reimer, U. Mikolajewicz, et al. (2001), Estimates of anthropogenic carbon uptake from four three-dimensional global ocean models, *Global Biogeochem. Cycles*, 15(1), 43-60.
- Ostlund, H. G. and M. Stuiver (1980), Geosecs Pacific Radiocarbon, *Radiocarbon*, 22(1), 25-53.
- Pacanowski, R. C., K. Dixon and A. Rosati (1993), The GFDL modular ocean model users guide, pp. 46, Geophysical Fluid Dynamics Laboratory, Princeton.
- Parker, R. L. and M. K. McNutt (1980), Statistics for the one-norm misfit measure, *J. Geophys. Res.*, 85, 4429-4430.
- Peacock, S. (2004), Debate over the ocean bomb radiocarbon sink: Closing the gap, *Global Biogeochem. Cycles*, 18, GB2022.
- Peacock, S., M. Maltrud and R. Bleck (2005), Putting models to the data test: a case study using Indian Ocean CFC-11 data, *Ocean Modelling*, 9(1), 1-22.
- Peng, T. H., W. S. Broecker, G. G. Mathieu, et al. (1979), Radon evasion rates in the Atlantic and Pacific Oceans as determined during the Geosecs Program, *Journal of Geophysical Research-Oceans and Atmospheres*, 84(NC5), 2471-2486.
- Perrie, W., W. Q. Zhang, X. J. Ren, et al. (2004), The role of midlatitude storms on air-sea exchange of CO₂, *Geophys. Res. Lett.*, 31(9).
- Plattner, G. K., F. Joos and T. F. Stocker (2002), Revision of the global carbon budget due to changing air-sea oxygen fluxes, *Global Biogeochem. Cycles*, 16(4), art. no.-1096.
- Potter, C. S., J. T. Randerson, C. B. Field, et al. (1993), Terrestrial ecosystem production - a process model based on global satellite and surface data, *Global Biogeochem. Cycles*, 7(4), 811-841.
- Prentice, I. C., G. D. Farquhar, M. J. R. Fasham, et al. (2001), The Carbon Cycle and Atmospheric Carbon Dioxide, in *Climate Change 2001 : The Scientific Basis : Contribution of Working Group I to the Third Assessment Report of the Intergovernmental Panel on Climate Change*, edited by J. T. Houghton, et al., pp. 183-238, Cambridge University Press, Cambridge, U.K. and New York.

- Primeau, F. (2005), Characterizing transport between the surface mixed layer and the ocean interior with a forward and adjoint global ocean transport model, *J. Phys. Oceanogr.*, 35(4), 545-564.
- Quay, P., S. King, D. White, et al. (2000), Atmospheric ^{14}C : A tracer of OH concentration and mixing rates, *J. Geophys. Res.*, 105(D12), 15147-15166.
- Quay, P., R. Sonnerup, T. Westby, et al. (2003), Changes in the $^{13}\text{C}/^{12}\text{C}$ of dissolved inorganic carbon in the ocean as a tracer of anthropogenic CO_2 uptake, *Global Biogeochem. Cycles*, 17(1), art. no.-1004.
- Randerson, J. T., I. G. Enting, E. A. G. Schuur, et al. (2002), Seasonal and latitudinal variability of troposphere $\Delta^{14}\text{CO}_2$: Post bomb contributions from fossil fuels, oceans, the stratosphere, and the terrestrial biosphere, *Global Biogeochem. Cycles*, 16(4), art. no. 1112.
- Roy, T., P. Rayner, R. Matear, et al. (2003), Southern hemisphere ocean CO_2 uptake: reconciling atmospheric and oceanic estimates, *Tellus*, 55(2), 701-710.
- Rozanski, K., I. Levin, J. Stock, et al. (1995), Atmospheric $^{14}\text{CO}_2$ variations in the Equatorial region, *Radiocarbon*, 37(2), 509-515.
- Rubin, S. I. and R. M. Key (2002), Separating natural and bomb-produced radiocarbon in the ocean: The potential alkalinity method, *Global Biogeochem. Cycles*, 16(4), art. no.-1105.
- Sabine, C. L., R. A. Feely, N. Gruber, et al. (2004), The oceanic sink for anthropogenic CO_2 , *Science*, 305(5682), 367-371.
- Schlitzer, R. (2000), Applying the adjoint method for biogeochemical modeling: export of particulate organic matter in the world ocean, in *Inverse Methods in Global Biogeochemical Cycles*, edited by P. Kasibhatla, et al., pp. 107-124, American Geophysical Union, Washington.
- Stammer, D., K. Ueyoshi, A. Köhl, et al. (2004), Estimating air-sea fluxes of heat, freshwater, and momentum through global ocean data assimilation, *J. Geophys. Res.*, 109, C05023, doi:10.1029/2003JC002082.
- Stephens, C., J. I. Antonov, M. E. Conkright, et al. (2002), *World Ocean Atlas 2001, Volume 1: Temperature*, 167 pp., US Government Printing Office, Washington.
- Stuiver, M. and B. Becker (1993), High-precision decadal calibration of the radiocarbon time scale, AD 1950-6000 BC, *Radiocarbon*, 35(1), 35-65.
- Stuiver, M. and H. G. Ostlund (1980), Geosecs Atlantic radiocarbon, *Radiocarbon*, 22(1), 1-24.
- Stuiver, M. and H. G. Ostlund (1983), Geosecs Indian-Ocean and Mediterranean radiocarbon, *Radiocarbon*, 25(1), 1-29.
- Stuiver, M. and H. A. Polach (1977), Reporting of C-14 data - Discussion, *Radiocarbon*, 19(3), 355-363.
- Stuiver, M. and P. D. Quay (1981), Atmospheric ^{14}C changes resulting from fossil fuel CO_2 release and cosmic ray flux variability, *Earth Planet. Sci. Lett.*, 53(3), 349-362.
- Suess, H. E. (1955), Radiocarbon Concentration in Modern Wood, *Science*, 122(3166), 415-417.
- Takahashi, T., S. C. Sutherland, C. Sweeney, et al. (2002), Global sea-air CO_2 flux based on climatological surface ocean $p\text{CO}_2$, and seasonal biological and temperature effects, *Deep-Sea Res.*, 49(9-10), 1601-1622.

- Tans, P. P., J. A. Berry and R. F. Keeling (1993), Oceanic $^{13}\text{C}/^{12}\text{C}$ observations: a new window on ocean CO_2 uptake, *Global Biogeochem. Cycles*, 7(2), 353-368.
- Tans, P. P., A. F. M. Dejong and W. G. Mook (1979), Natural atmospheric C-14 variation and the Suess Effect, *Nature*, 280(5725), 826-827.
- Tans, P. P., I. Y. Fung and T. Takahashi (1990), Observational constraints on the global atmospheric CO_2 Budget, *Science*, 247(4949), 1431-1438.
- Thompson, M. V. and J. T. Randerson (1999), Impulse response functions of terrestrial carbon cycle models: method and application, *Glob. Change Biol.*, 5(4), 371-394.
- Toggweiler, J. R., K. Dixon and K. Bryan (1989), Simulations of radiocarbon in a coarse-resolution world ocean model .1. Steady state prebomb distributions, *J. Geophys. Res.*, 94(C6), 8217-8242.
- Trolier, M., J. W. C. White, P. P. Tans, et al. (1996), Monitoring the isotopic composition of atmospheric CO_2 : Measurements from the NOAA Global Air Sampling Network, *J. Geophys. Res.*, 101(D20), 25897-25916.
- Turney, D. E., W. C. Smith and S. Banerjee (2005), A measure of near-surface fluid motions that predicts air-water gas transfer in a wide range of conditions, *Geophys. Res. Lett.*, 32(4).
- Van Scoy, K. A., K. P. Morris, J. E. Robertson, et al. (1995), Thermal skin effect and the air-sea flux of carbon dioxide: A seasonal high-resolution estimate, *Global Biogeochem. Cycles*, 9(2), 253-262.
- Vogel, J. C. (1971), Pretoria radiocarbon dates I, *Radiocarbon*, 13(2), 378-394.
- Walsh, J. (1978), A data set on northern hemisphere sea ice extent, 1953-1976, pp. 49-51, World Data Center for Glaciology (Snow and Ice), Report GD-2.
- Wanninkhof, R. (1992), Relationship between wind-speed and gas-exchange over the ocean, *J. Geophys. Res.*, 97(C5), 7373-7382.
- Wanninkhof, R. and W. R. McGillis (1999), A cubic relationship between air-sea CO_2 exchange and wind speed, *Geophys. Res. Lett.*, 26(13), 1889-1892.
- Wanninkhof, R., K. F. Sullivan and Z. Top (2004), Air-sea gas transfer in the Southern Ocean, *J. Geophys. Res.*, 109(C8).
- Ward, B., R. Wanninkhof, W. R. McGillis, et al. (2004), Biases in the air-sea flux of CO_2 resulting from ocean surface temperature gradients, *J. Geophys. Res.*, 109(C8).
- Weiss, R. F. and B. A. Price (1980), Nitrous oxide solubility in water and seawater, *Mar. Chem.*, 8(4), 347-359.
- Woolf, D. K. (2005), Parametrization of gas transfer velocities and sea-state-dependent wave breaking, *Tellus*, 57(2), 87-94.
- Wunsch, C. (1996), *The Ocean Circulation Inverse Problem*, 442 pp., Cambridge University Press, Cambridge; New York.
- Zhang, J., P. D. Quay and D. O. Wilbur (1995), Carbon isotope fractionation during gas-water exchange and dissolution of CO_2 , *Geochim. Cosmochim. Acta*, 59(1), 107-114.
- Zhao, D., Y. Toba, Y. Suzuki, et al. (2003), Effect of wind waves on air-sea gas exchange: proposal of an overall CO_2 transfer velocity formula as a function of breaking-wave parameter, *Tellus*, 55(2), 478-487.
- Zwally, H. J., J. Comiso, C. Parkinson, et al. (1983), Antarctic Sea Ice, 1973-1976: Satellite Passive Microwave Observations, pp. 206, NASA.